RECORD 2021/9

GEOPHYSICAL ANALYSIS OF BARNICARNDY 1: DATA QUALITY CONTROL, VELOCITY ANOMALIES, OUT-OF-PLANE REFLECTIONS, AND CORRELATION UNCERTAINTIES

by
Y Zhan

Government of **Western Australia**
Department of **Mines, Industry Regulation and Safety**

Geological Survey of Western Australia

Government of **Western Australia**
Department of **Mines, Industry Regulation and Safety**

RECORD 2021/9

GEOPHYSICAL ANALYSIS OF BARNICARNDY 1: DATA QUALITY CONTROL, VELOCITY ANOMALIES, OUT-OF-PLANE REFLECTIONS, AND CORRELATION UNCERTAINTIES

by

Y Zhan

PERTH 2021

Geological Survey of Western Australia

MINISTER FOR MINES AND PETROLEUM
Hon Bill Johnston MLA

DIRECTOR GENERAL, DEPARTMENT OF MINES, INDUSTRY REGULATION AND SAFETY
Richard Sellers

EXECUTIVE DIRECTOR, GEOLOGICAL SURVEY AND RESOURCE STRATEGY
Jeff Haworth

REFERENCE
The recommended reference for this publication is:
Zhan, Y 2021, Geophysical analysis of Barnicarndy 1: data quality control, velocity anomalies, out-of-plane reflections, and correlation uncertainties: Geological Survey of Western Australia, Record 2021/9, 24p.

ISBN 978-1-74168-942-6
ISSN 2204-4345

Grid references in this publication refer to the Geocentric Datum of Australia 1994 (GDA94). Locations mentioned in the text are referenced using Map Grid Australia (MGA) coordinates, Zone 50. All locations are quoted to at least the nearest 100 m.

Based on consultation with the Western Desert Lands Aboriginal Corporation (WDLAC) on the cultural significance of the name, Waukarlycarly, it has been agreed to change the name of the well to Barnicarndy 1 and the tectonic subdivision to Barnicarndy Graben. This and all future publications will now refer to the Barnicarndy 1 stratigraphic drillhole (previously Waukarlycarly 1) and the Barnicarndy Graben (previously Waukarlycarly Embayment).

Published 2021 by the Geological Survey of Western Australia
This Record is published in digital format (PDF) and is available online at <www.dmirs.wa.gov.au/GSWApublications>.

Further details of geoscience products are available from:
Information Centre
Department of Mines, Industry Regulation and Safety
100 Plain Street
EAST PERTH WESTERN AUSTRALIA 6004
Telephone: +61 8 9222 3459 Email: publications@dmirs.wa.gov.au
www.dmirs.wa.gov.au/GSWApublications

Cover image: Wave and wind sculpted stromatolites at Flagpole Landing, Hamelin Pool in the world heritage site of Shark Bay, Western Australia (photo courtesy of Heidi Allen, DMIRS)

Contents

Figures

Tables

Appendix

Geophysical analysis of Barnicarndy 1: data quality control, velocity anomalies, out-of-plane reflections, and correlation uncertainties

by

Y Zhan

Abstract

Barnicarndy 1 was drilled as a stratigraphic well to a total depth of 2680.53 m near the south-southeast end of the eponymous graben of the Canning Basin in 2019 and was located on the 18GA–KB1 Kidson deep seismic survey. The well penetrated 2585 m of dominantly clastic sedimentary rocks with an angular unconformity above a slightly metamorphosed and weakly deformed Proterozoic dolomite basement. The post-drilling data exhibit several anomalies and inconsistencies, including ultra-slow velocity of the vertical seismic profile (VSP) within the top 210 m and substantially high velocity from 210 to 1392 m, resulting in poor synthetic seismic correlation and discrepancies between the estimated and actual depths. The VSP shows that the uppermost sedimentary section has an average velocity of less than 1000 m/s, which is unrealistically slow and probably caused by a systematic time delay in the data acquisition. Such delaying effect is removed by calculating the VSP interval velocity, which has reasonable consistency with the sonic velocity and lithological packages. This consistency verifies that the interval from 210 to 1392 m has high velocities that are beyond the range of offset wells at equivalent depths and does not follow an expected trend along most of the well trajectory.

Quantitative analyses of multiple synthetic correlations suggest that the VSP requires a 215 ms upwards shift to achieve optimal synthetic correlation with the seismic section. Based on the optimal seismic correlation, the depth discrepancies in the pre-drilling prognosis are not related to pre-drilling seismic interpretation, as the two-way time (TWT) picks for major boundaries mostly match what has been penetrated in Barnicarndy 1. Two-thirds of the depth error for basement prognosis comes from the unexpected high velocity in the shallow formations. The velocity anomalies indicate that the Barnicarndy Graben possibly has a complex history of tectonic movement and thick sections could have been eroded during the Late Triassic. The remaining discrepancy in depth prognosis for the basement is related to out-of-plane seismic reflection near the south-southeast end of the embayment. The steeply dipping basement causes out-of-plane issues for 2D seismic data, such that the 18GA–KB1 Kidson seismic survey images the shallower basement reflected from further south, rather than what is vertically below the acquisition points.

KEYWORDS: Barnicarndy Graben, out-of-plane, seismic interpretation, sonic, tectonic movement, VSP

Introduction

The Paleozoic to Mesozoic Canning Basin in northern Western Australia has been a focus of exploration for petroleum and Mississippi Valley-type lead–zinc mineralization since the early 1920s. With the increase of drilling and seismic data, the understanding of the basin geology has been gradually enhanced in prospective and accessible regions such as the Lennard Shelf and the Admiral Bay Fault Zone between the Willara Sub-basin and the Broome Platform (Fig. 1a). However, much of the basin remains poorly understood due to lack of well penetrations, such as the Kidson and Gregory Sub-basins towards the inland near the Western Australia – Northern Territory border, as well as the Barnicarndy Graben and the Wallal Embayment in the southern periphery of the Canning Basin.

Barnicarndy 1 was the first well drilled in the Barnicarndy Graben, as a joint project between the Geological Survey of Western Australia (GSWA) and Geoscience Australia (GA). Funding was primarily from the Exploring for the Future initiative (EFTF) of the Commonwealth Government with assistance from the Exploration Incentive Scheme (EIS) of the Western Australian State Government. Based on consultation with the Western Desert Lands Aboriginal Corporation regarding the cultural significance of the name Waukarlycarly, it has been agreed to change the name of the well to Barnicarndy 1 and the tectonic subdivision to Barnicarndy Graben. This and all future publications will now refer to the Barnicarndy 1 stratigraphic drillhole (previously Waukarlycarly 1) and the Barnicarndy Graben (previously Waukarlycarly Embayment).

The objective of the well was to provide stratigraphic data and improve the understanding of this isolated tectonic element of the Canning Basin, which in 2018 had been imaged by the Kidson deep seismic survey (18GA–KB1; Southby et al., 2019; Zhan and Haines, 2021). The well was situated about 50 m to the south-southwest of the seismic acquisition route (Telfer Mine Road) and had a minimal deviation with its bottom landed directly underneath the road. The drilling revealed different packages of lithologies from the rest of the basin, including thick, porous sandstones, claystone, as well as sand- or mud-dominated diamictite. Although a high level of mismatch is commonly found in wildcat exploration wells between prognosis and

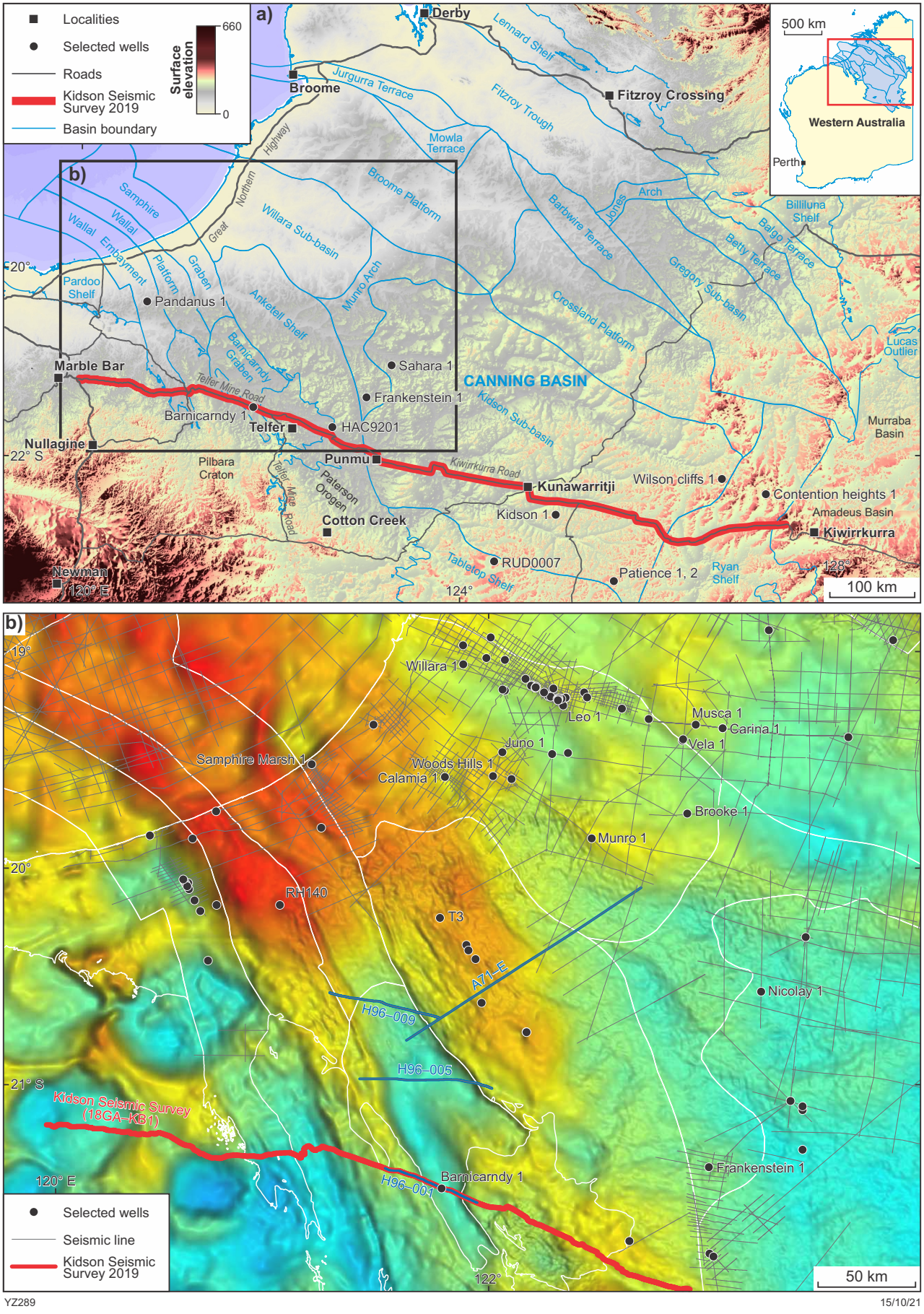

YZ289 15/10/21

Figure 1. Location map of Barnicarndy 1 and Kidson seismic survey: a) tectonic elements of the Canning Basin (GSWA, 2017) and digital elevation model; b) seismic lines and drillholes superimposed on gravity image (GSWA, 2020)

actual formation depths, the thickness of the Paleozoic infill in Barnicarndy 1 was considerably underestimated based on time interpretation on the 2D seismic section and velocity from offset wells. Inconsistencies between wireline logs, the vertical seismic profile (VSP; see Appendix), synthetic seismograms and seismic reflection data prompted a detailed investigation to reconcile the seismic interpretation with the post-drilling results.

Geological background

Canning Basin

The Canning Basin, a mostly onshore intracratonic basin covering 640 000 km^2, contains an Ordovician to Cretaceous sedimentary succession reaching an estimated maximum thickness of 15 km in the Fitzroy Trough (Forman and Wales, 1981; Kennard et al., 1994; Fig. 1a). The basin is subdivided into several major elements (GSWA, 2017) that include: 1) an elongate northwesterly trending depocentre (the Fitzroy Trough and contiguous Gregory Sub-basin); 2) a mid-basin platform (the Broome and Crossland Platforms); 3) southern depocentres (the Willara and Kidson Sub-basins). The periphery of the basin is flanked by the Pardoo – Anketell – Tabletop Shelves to the south, the Lennard – Billiluna Shelves to the north, and the Ryan Shelf to the east (Fig. 1a). The southern Canning Basin was estimated to have a maximum thickness of 10 km in the Kidson Sub-basin and Ryan Shelf (Frogtech, 2017). Most of the succession in the southern Canning Basin was deposited during the Ordovician to Permian (Forman and Wales, 1981; Haines, 2011), with possibility of the Cambrian strata in the lower part of the sedimentary succession.

Barnicarndy Graben

The Barnicarndy Graben is considered part of the Canning Basin, but is distinctly separated by faults from the main depocentres (Willara and Kidson Sub-basins) in the southwestern peripheral area of the basin. It was first identified through Bouguer gravity data, which show a local gravity low within a regional north-northwesterly trending gravity high (the Anketell Regional Gravity Ridge in Fraser, 1976, or Warri Gravity Ridge in Iasky, 1990). This gravity low implied the presence of a basinal depression between the Pilbara Craton and the Canning Basin. The gravity low is about 25–50 km wide and 150 km long, subparallel to the adjacent Precambrian structural trends in the Paterson Orogen (Figs 1b, 2).

The graben configuration was later confirmed by four seismic lines broadly normal to the strike of the graben (Fig. 1b): one in the north acquired by WAPET (A71–E; Allen et al., 1971), and the remaining three by Hunt Oil Company (H96–001, 005 and 009; Hunt Oil Company of Australia, 1997). Line H96–001 in the south-southeast of the graben was re-surveyed by Geoscience Australia in conjunction with Geological Survey of Western Australia as a part of the Kidson seismic survey 18GA–KB1 (Southby et al., 2019; Carr et al., 2020; Zhan and Haines, 2021). These seismic lines show that the graben is fault-bounded to the Paterson Orogen and the Anketell Shelf (Fig. 1a).

The sedimentary rocks within the graben were unknown prior to the drilling of Barnicarndy 1. The Permian and younger cover was interpreted to be widespread (Hocking, 1994a,b) and extended from the main part of the Canning Basin in the north. The thick section beneath the Permian with a highly reflective seismic signature was uncertain in its age but was either interpreted as Proterozoic infill with a thin Ordovician component overlying crystalline basement (Hunt Oil Company of Australia, 1997) or as a Lower Paleozoic section equivalent to the Ordovician–Silurian near the southern margin of the Willara and Kidson Sub-basins (Roach et al., 2010; Alavi, 2013).

Pre-drilling well prognosis

Seismic interpretation

The Kidson Sub-basin seismic survey crosses the Barnicarndy Graben and was used for pre-drill interpretation (Figs 1, 2). The final seismic datum was placed at 500 m above mean sea level (MSL), which is above the highest surface elevation (480 m) in order to preserve the data in the elevated areas. Static corrections were applied to the seismic data to compensate for the effects of variations in elevation, weathering thickness and velocity. A replacement velocity of 2500 m/s was used between the near-weathering floating datum and the final datum. The final processed data retained its recording polarity and was output with a minimum phase polarity (Velseis, 2019).

The sedimentary successions in the Barnicarndy Graben were difficult to identify from the Kidson seismic survey 18GA–KB1, especially the thick section below the interpreted Permian rocks due to the lack of wells. Therefore, the seismic interpretation for the pre-drill well prognosis only confidently included three major horizons: Base Mesozoic, Base Permian and Top basement. However, four pre-Permian formation boundaries above the Top basement (Fig. 3), with lower confidence: the top of the Nita, Goldwyer, Willara and Nambeet Formations, were tentatively prognosed, given their widespread presence outside of the graben in the southern Canning Basin (Zhan, 2018).

Based on the comparison of three isolated subparallel seismic lines within the graben, the Top basement was interpreted as a roughly flat-lying reflector with significant vertical displacement across the boundary faults. The basement horizon appears to shallow towards the eastern boundary fault, but this apparent effect is related to the obliqueness of the line and the shallowing trend to the south-southeast along the strike of the embayment (Figs 2, 3).

From 0.35 to 0.45 s two-way time (TWT) within the graben, the seismic profile shows an angular unconformity that truncates the reflectors underneath (Fig. 3), providing evidence of possible Permian glacial or fluvial erosion. This angular contact in the shallow section is a typical signature of the Base Grant Group unconformity in other parts of the Canning Basin (Zhan and Mory, 2013; Zhan 2017, 2018, 2019) and is interpreted as Base Permian in the Barnicarndy Graben. The upper-most seismic reflector smoothly extends across the boundary faults towards the Anketell Shelf and Paterson Orogen and is possibly the

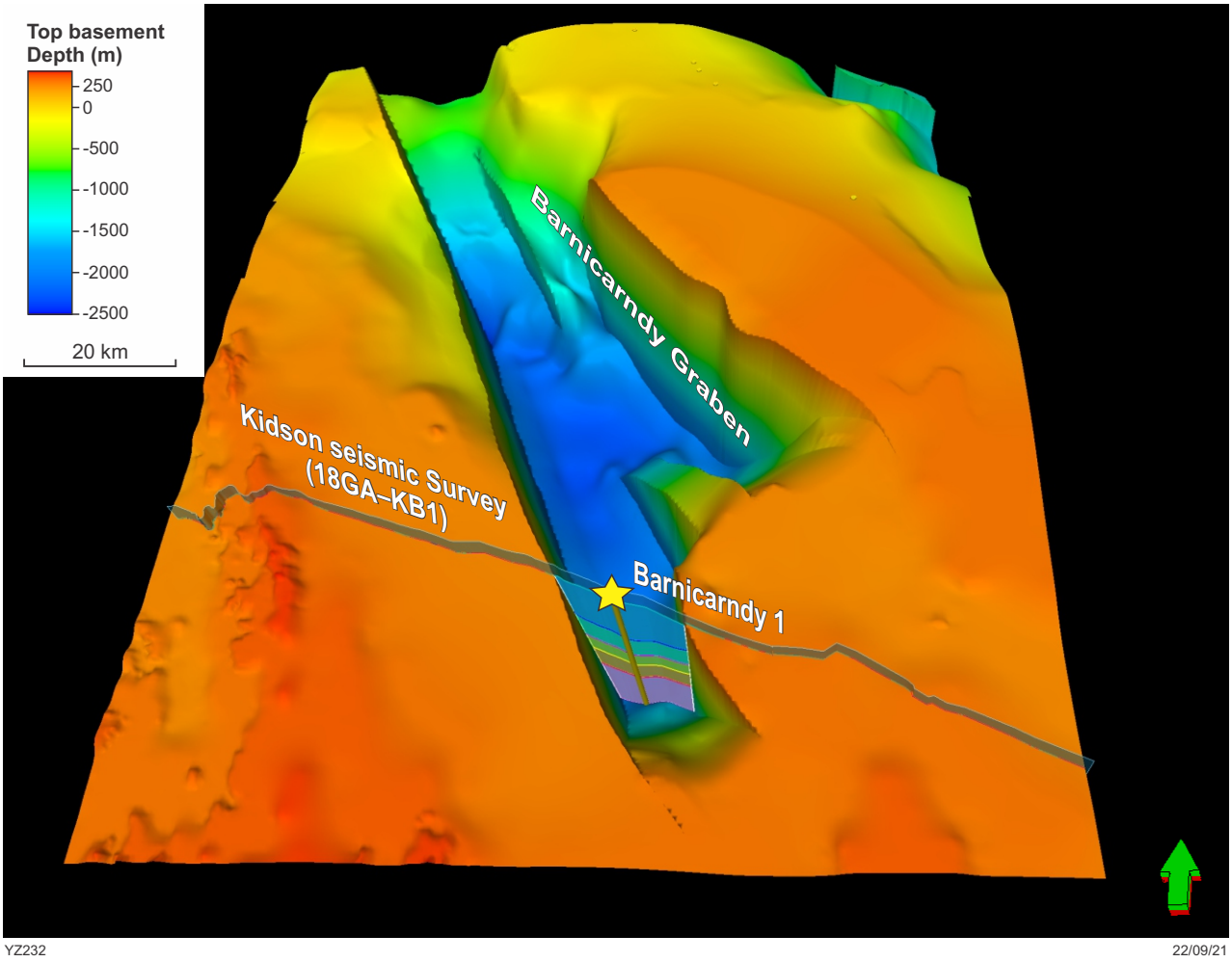

Figure 2. 3D model of the Barnicarndy Graben, showing the position of the Barnicarndy 1 well and the Kidson seismic survey. The model is based on three seismic profiles across the graben, gravity and magnetic data, as well as Precambrian outcrops outside of the graben

interface between unconsolidated Mesozoic–Cenozoic cover and Permian strata. Between the Base Permian and Top basement horizons, the Carribuddy Group and the Nita, Goldwyer, Willara and Nambeet Formations were assumed to be present in the Barnicarndy Graben. These formation boundaries were interpreted where seismic events separate continuous high-amplitude packages from less reflective zones (Fig. 3).

Velocity analysis and depth conversion

Due to the lack of well penetrations, the depth conversion is based on either the seismic stacking velocity inside the Barnicarndy Graben or offset wells beyond the graben in the southern Canning Basin. The stacking velocity is picked on semblance profiles to find the best fit on common depth point seismic gathers. This velocity translates the travel time from all traces with different offsets onto the same vertical trace, allowing the reflection off the same subsurface point from different travel paths to be stacked together to provide a single vertical trace for geological interpretation. The stacking velocities can be converted into average or interval velocities using the Dix equation (Dix, 1955), but they may bear little relation to the actual geological information because the stacking velocities were picked to improve signal-to-noise ratio and make the assumption of a flat-lying surface. The Kidson seismic survey 18GA–KB1 was depth migrated after six iterations of the velocity model (Fig. 4; Velseis, 2019). However, due to the long distance between the seismic line and pre-existing wells, such as 60 km to Frankenstein 1, 15 km to Kidson 1 and 75 km to Patience 2 (Fig. 1b), the interval velocity model of depth migration derived from stacking velocity was not calibrated to the well velocities (Velseis, 2019). The depth migrated seismic section shows the Top basement in Barnicarndy 1 at about 2800 m below the surface (about 2550 m below the MSL in Figure 4a).

The interval velocities for the depth migration appear to be considerably faster than expected as shown by comparison of the time–depth relationship at the intersection common depth point (CDP) 51411, where Frankenstein 1 can be correlated to the Kidson seismic line (Fig. 5). At this intersection, 1.27 s TWT (Point A in Figure 5) below seismic datum MSL (0 s TWT) is equivalent to 2650 m below MSL based on the seismic depth migration data. However, the VSP in Frankenstein 1 (Command Petroleum NL, 1989) indicates that 1.36 s TWT (Point B; below MSL) corresponds to 2379 m below MSL. Therefore, the depth comparison

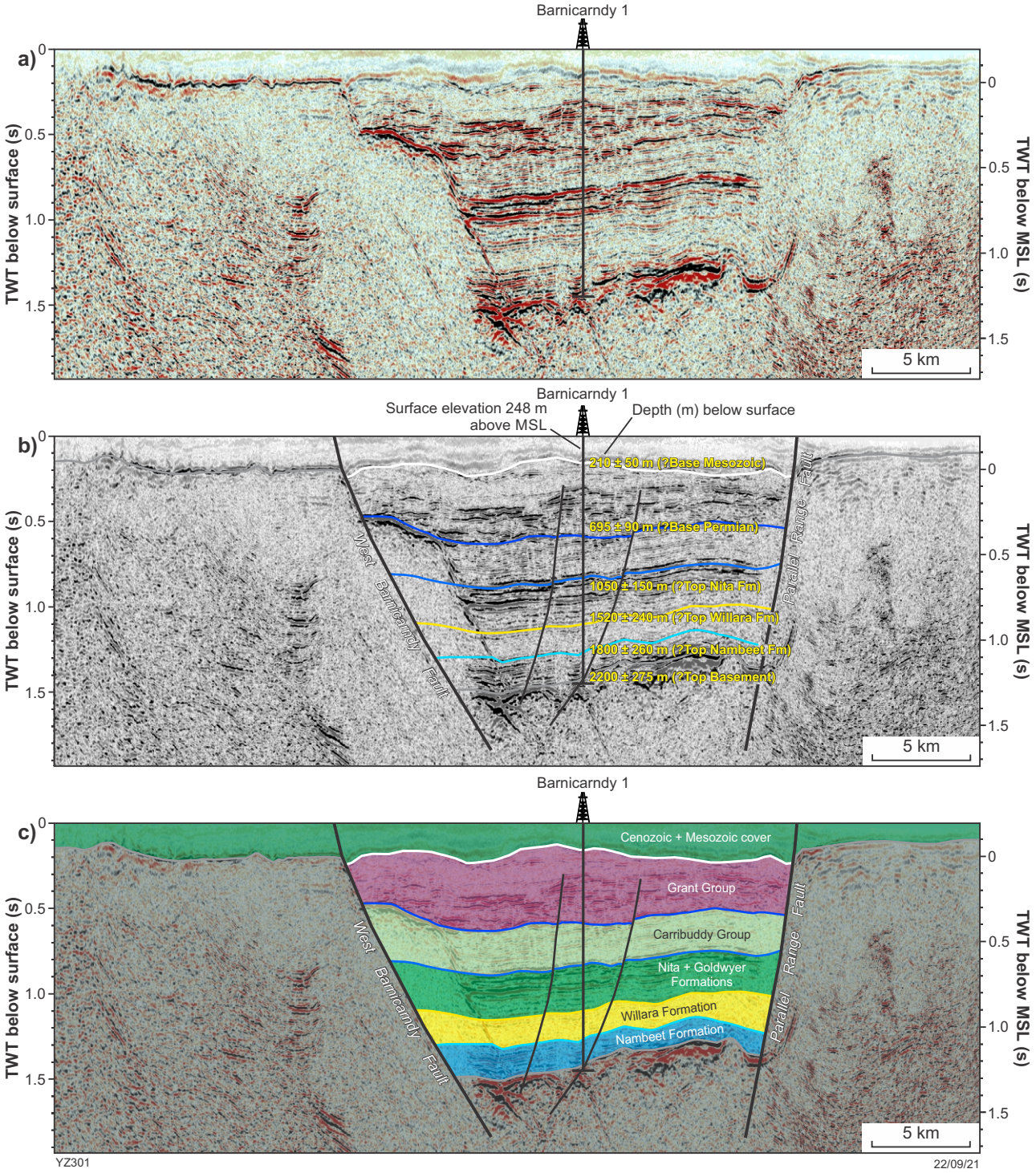

Figure 3. Pre-drilling seismic interpretation and depth prognosis for Barnicarndy 1, with vertical axes marking TWT below surface (left axis; 0 s = ground level at well site) and TWT below mean sea level (right axis; 0 s = MSL along seismic profile): a) uninterpreted seismic section; b) seismic interpretation with depth prognosis; c) predicted geological section

at CDP 51411 shows that Point A, being 90 milliseconds (ms) shallower (1.27 s vs 1.36 s) in TWT, is inversely 271 m deeper than Point B (2650 m vs 2379 m) on the depth profile. This discrepancy casts doubt in using the depth migration velocity or directly applying pre-stack depth migration profile for well prognosis. For this reason, the pre-spud prognosis used the time migration data for seismic interpretation and applied velocities from offset wells for depth conversion at the predicated formation boundaries. The application of the offset well velocity is also based on the assumption that the Barnicarndy Graben is geologically comparable to the Willara and Kidson Sub-basins.

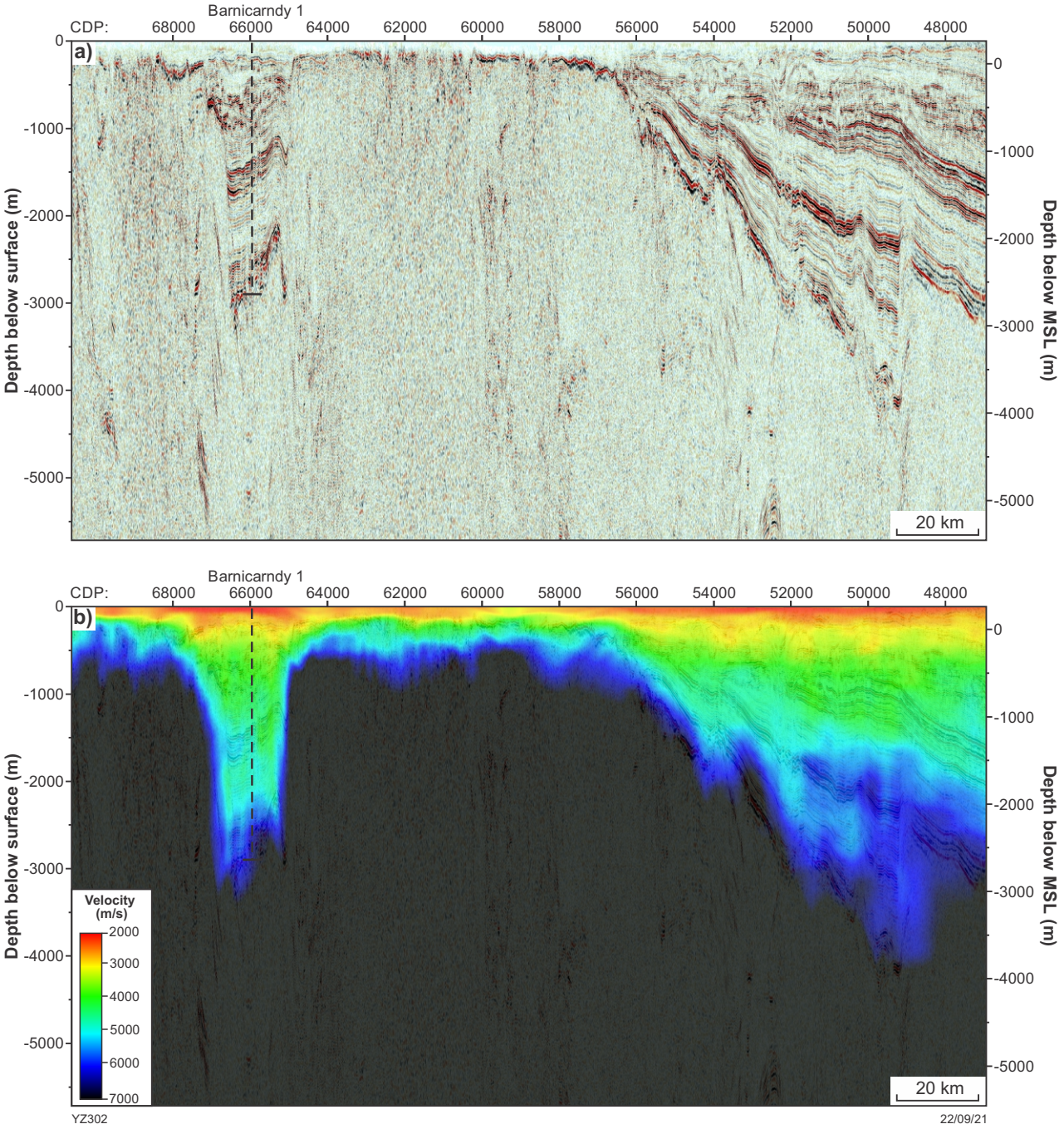

Figure 4. Pre-stack depth migration (PSDM) velocity between the Barnicarndy Graben and Kidson Sub-basin: a) PSDM seismic section; b) seismic depth section overlain by interval velocity

The time–depth relationships (Fig. 6), derived from offset wells that are mostly based on their VSPs, show a broad range of velocities from slow in Munro 1, to medium in Willara 1 and fast in Frankenstein 1 (Fig. 6). The wide range produces significant depth variations for the same time picks. For example, the differences from applying the time–depth of Munro 1 as compared to Frankenstein 1 are about 440 m at TWT 0.8 s, 500 m at 1 s and 550 m at 1.2 s. The reasons for the broad velocity range are probably the variation in stratigraphy between these wells and differences in tectonic history; that is, burial, uplift and erosion in the different regions of the Canning Basin. For instance, there was over 500 m of salt penetrated in Frankenstein 1 and 600 m of limestone in Willara 1. These two lithologies commonly have much faster velocities than clastic sedimentary rocks at similar depths. Below the major unconformities, such as the Base Permian, the same burial depth with different amounts of erosion can lead to different compaction, and therefore variations in density and porosity, and therefore velocity differences. The different geological scenarios were difficult to apply in the Barnicarndy Graben due to lack of well penetrations prior to drilling Barnicarndy 1. Thus the pre-drill velocity prognosis used an averaged velocity curve derived from wells in the Kidson and Willara

Sub-basins and the Broome Platform. The uncertainties increase with depth to around ±275 m contingency error margin at Top basement to allow for uncertainties from the unknown stratigraphy.

Because the topography varies significantly between offset wells, the pre-drilling analysis of the velocity used ground level and MSL as separate datums to calculate the velocity range of the offset wells (Fig. 6a,b). The MSL at Barnicarndy 1 is estimated at about 200 ms below the ground level, based on the final seismic datum at 500 m above MSL, the replacement velocity of 2500 m/s (as per the processing report), and the measured surface elevation at 258 m above MSL (Velseis, 2019). The top of the basement is interpreted at ~1.42 s below the ground level, which is equivalent to ~1.22 s below the MSL seismic datum at 0 s on the seismic sections. This basement TWT pick can be directly converted to a depth between 1940 and 2340 m below the ground level based on the offset wells (Fig. 6a). The TWT below MSL in the offset wells corresponds to a wider range of 1630–2150 m below MSL (Fig. 6b), equivalent to 1890–2410 m below the ground level in Barnicarndy 1. Both calculations (1940–2340 m in Figure 6a, and 1890–2410 m in Figure 6b) yield a similar mean value at 2150 m for the Top basement pre-drill prognosis.

The seismic data shows a non-reflective interval in the lower part of the embayment, which indicates the possible presence of a salt layer similar to Frankenstein 1, which is the nearest well to Barnicarndy 1 (130 km), compared to 180 km to Nicolay 1 and 190 km to Munro 1. Therefore, the pre-drill depth prognosis of the basement in Barnicarndy 1 was revised to 2200 m below ground level (Table 1), with a greater weight being given to the Frankenstein 1 data.

Post-drilling velocity analysis

Barnicarndy 1 penetrated 2585 m of Paleozoic sedimentary rocks that consist of mostly sandstone and mudstone without any salt or thick carbonate intervals. Clastic intervals empirically have slow velocities and should have resulted in a shallower basement. However, the actual depths of the formation tops are increasingly deeper compared to prediction, with the Top basement (2585 m) calibrated to a non-reflective interface at 1.7 s TWT via VSP data. This calibration is inconsistent with the wireline logs, synthetic seismograms and seismic reflection data. The post-drill analysis uses the surface level as reference datum unless specifically stated as below MSL.

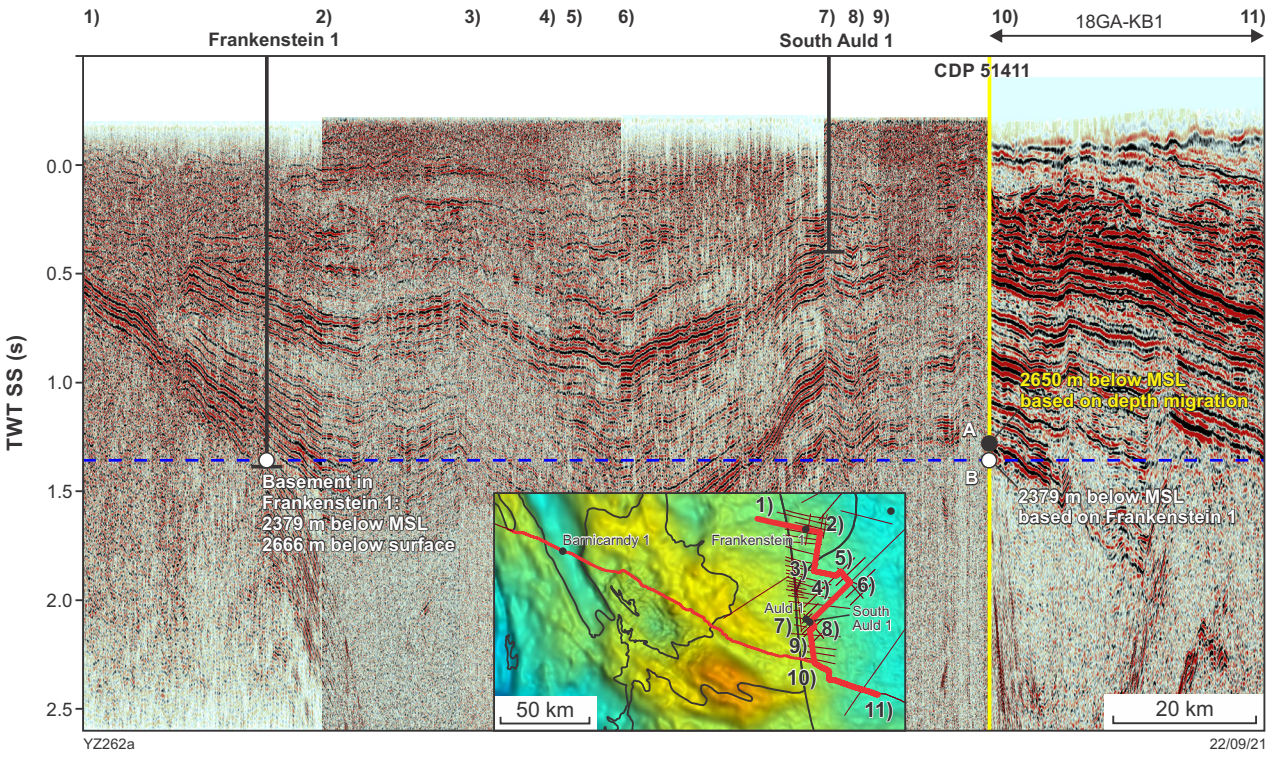

Figure 5. Depth comparison at intersection CDP 51411 on Kidson seismic profile. It shows that Point A, an interpreted basement at CDP 51411, is about 2650 m below MSL (2900 m below surface) based on the pre-stack depth migration section, and Point B is equivalent to the Top basement in Frankenstein 1 at 2379 m below MSL. However, the TWT section shows that Point A is about 1.27 s and is 90 ms shallower than Point B at ~1.36 s. This leads to a discrepancy between depth and time sections that Point A being 90 ms shallower in TWT but is 271 m deeper on the depth section. This discrepancy reduces confidence to use the depth migration velocity or directly apply the depth migration section for well prognosis

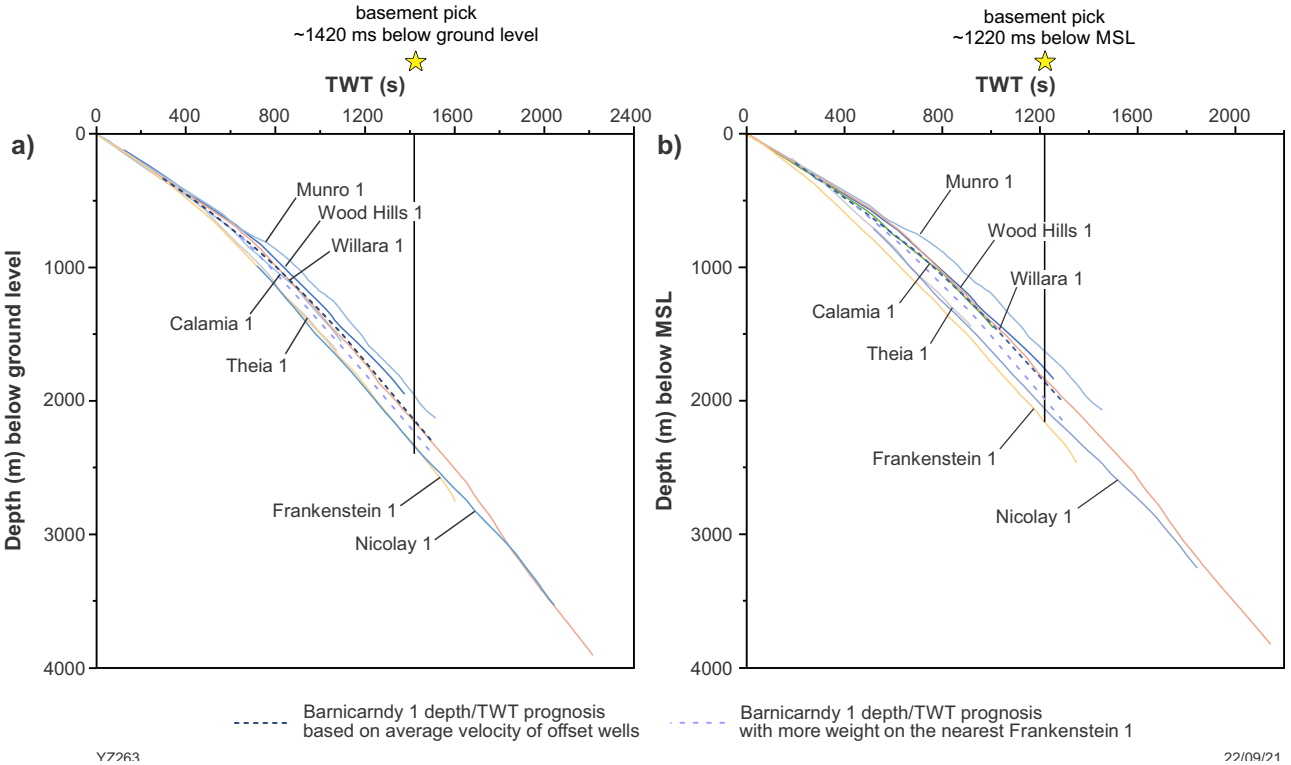

Figure 6. Time–depth pairs of offset wells from VSP and checkshot surveys: a) TVD vs TWT below surface; b) True vertical depth sub-sea (TVDSS) vs two-way time sub-sea (TWTSS) below MSL. Note the locations of the offset wells are marked in Figure 1b

Table 1. Barnicarndy 1 formation depth prognosis. Note the uncertainty is only based on the broad range of the velocity and does not include any errors from seismic interpretation that is difficult to quantify prior to the drilling

Formation pick	*TWT below surface (s)*	*TWT below MSL (s)*	*Depth below surface (m)*	*Uncertainties (m)*
?Base Mesozoic	0.16	−0.04	210	±50
?Base Permian	0.6	0.4	695	±90
?Top Nita Fm	0.84	0.64	1050	±150
?Top Willara Fm	1.15	0.92	1520	±240
?Top Nambeet Fm	1.25	1.05	1800	±260
?Top basement	1.42	1.22	2200	±275

Wireline logs

Wireline data (Figs 7, 8) were acquired under openhole conditions with three logging intervals: 216–727 m and 726–1603 m by Wireline Service Group (using a monopole detector), and 1603–2679 m by Weatherford with a dipole tool. In addition, each interval also covers a one-metre cased section above the openhole, so the readings in the casing provide reference for data calibration for log processing. The wireline logs include gamma ray, sonic, density, resistivity, neutron and others. These data mostly show reasonable changes at lithological boundaries (Fig. 8). For example, at 370 m, where the lithology changes downhole from siltstone to sandstone, the wireline responses show a decrease in the gamma ray, a sharp decrease in delta-T on the compressional sonic log representing an increase in velocity (Fig. 8), and a sudden increase in the separation between the shallow and deep resistivity indicating drilling mud invasion in the sandstone. These characteristics are consistent with typical wireline signatures between the siltstone and the sandstone units.

The wireline sonic velocity is distinctly different from those of the offset wells, which generally show an increase in velocity with depth (see the comparison in Figure 9). Barnicarndy 1 has high velocity at shallow depths, such as 3000 m/s at 210 m (~48 m above MSL), 3500 m/s at 450 m and 4200 m/s at 850 m. These sonic velocities are approximately 500–1000 m/s faster than other wells at equivalent depths (Fig. 9). It is likely that the high velocity

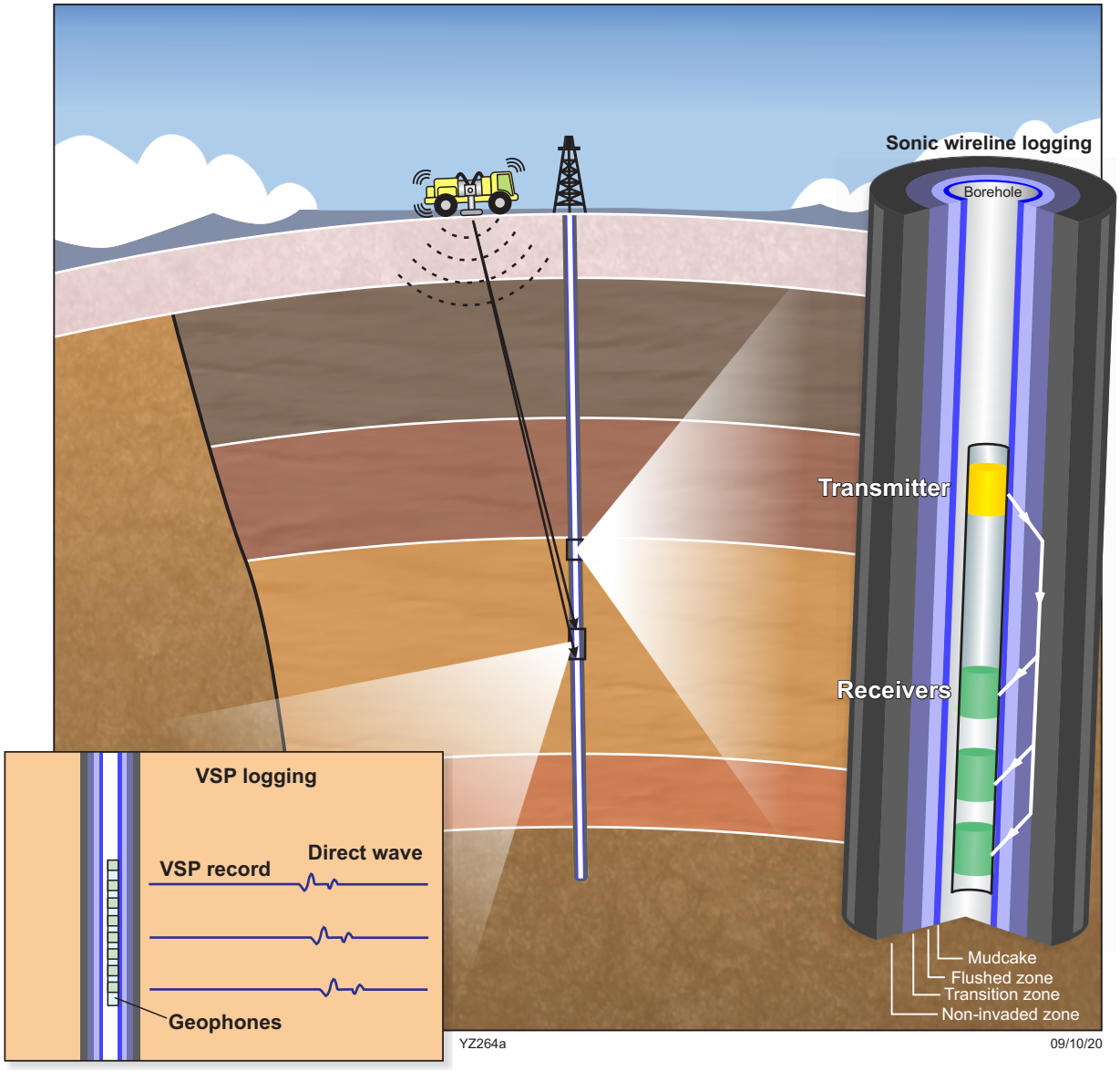

Figure 7. Schematic diagram for VSP logging (left) and sonic wireline logging (right) in Barnicarndy 1

extends upwards into the unlogged section below the weathering layer at 96 m. The thick claystone from 1345 to 2270 m has a slightly lower velocity (3900 m/s; Fig. 8) compared to 4000 m/s in the offset wells. This can be accounted for by the presence of high-velocity halite and carbonate at depth in the offset wells. The anomalous velocity profile indicates that the Grant Group section has been more widespread and deeply buried within the southwestern margin of the Canning Basin, than at present (Zhan and Haines, 2021). The thick Grant Group section was subjected to variable amounts of uplift and erosion, such as complete removal in the Telfer mining area and partial erosion in the Anketell Shelf and the Barnicarndy Graben areas, due to regional tectonism and fault reactivation during the Late Triassic (Zhan and Haines, 2021).

VSP and checkshot surveys

A zero-offset VSP (Figs 7, 10) was acquired by HiSeis using a two-level Sercel slimware system with 10 m spacing geophones (Kopty, 2020). The survey utilized one vibroseis truck as the energy source to generate two sweeps for every logging depth and used a surface geophone to ensure timing integrity. The VSP data was collected in various borehole conditions: in openhole between 1600 and 2620 m, through PQ casing between 727 and 1600 m, and through PQ and SQ casings between 650 and 727 m (Normore and Rapaic, 2020). The VSP first arrivals have excellent quality over the openhole section and show a distinctive arrival event between 0.6 s and 0.85 s one-way time (OWT; Fig. 10).

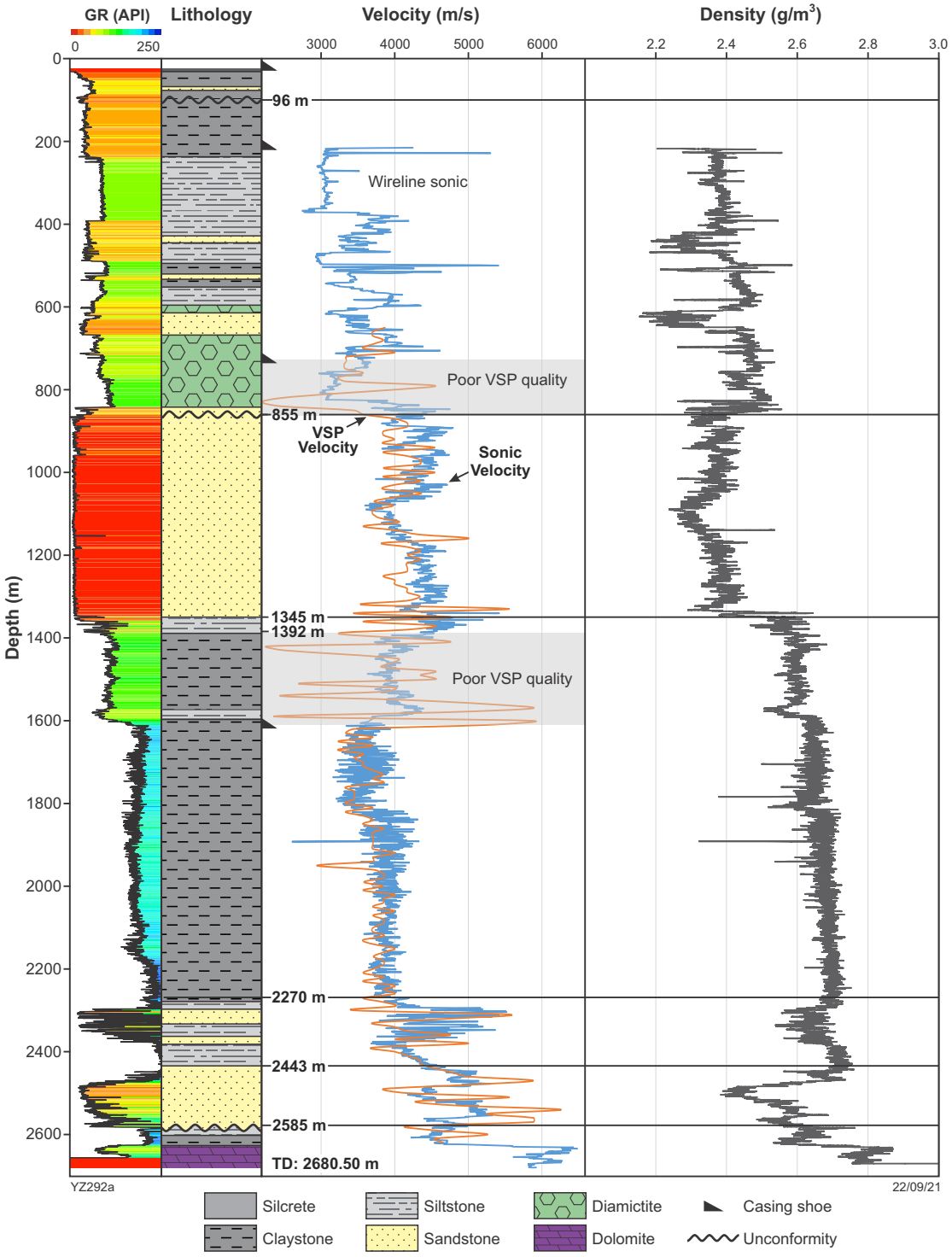

Figure 8. Wireline density (grey), sonic velocity (blue; converted from sonic slowness), and VSP interval velocity (red) compared alongside a generalized stratigraphic column for Barnicarndy 1

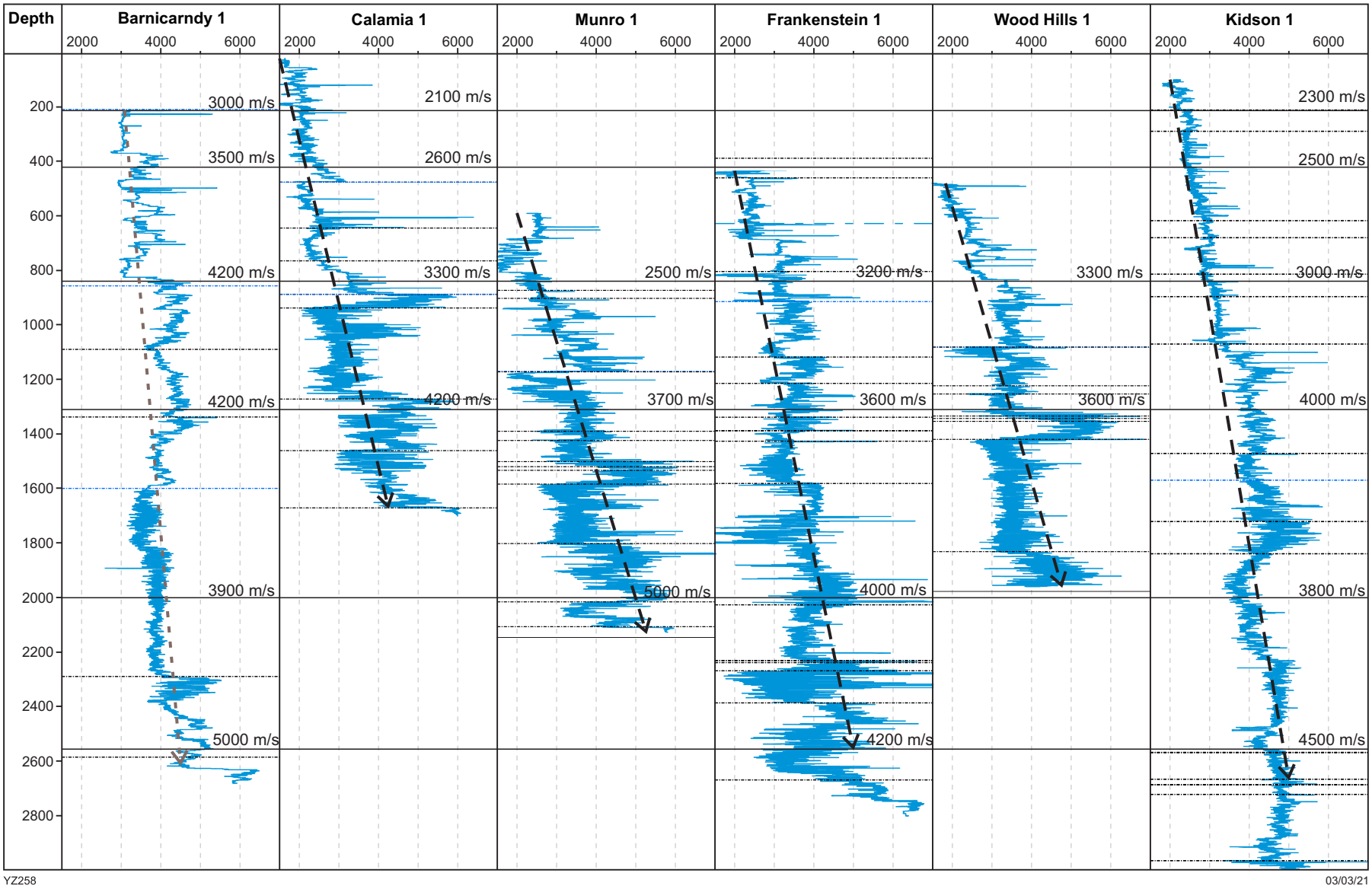

Figure 9. Sonic velocity comparison between Barnicarndy 1 and offset wells. The velocity in Barnicarndy 1 is unexpectedly high at shallow depths and has a lower velocity increase with depth than other wells (gradient of dashed lines with arrows)

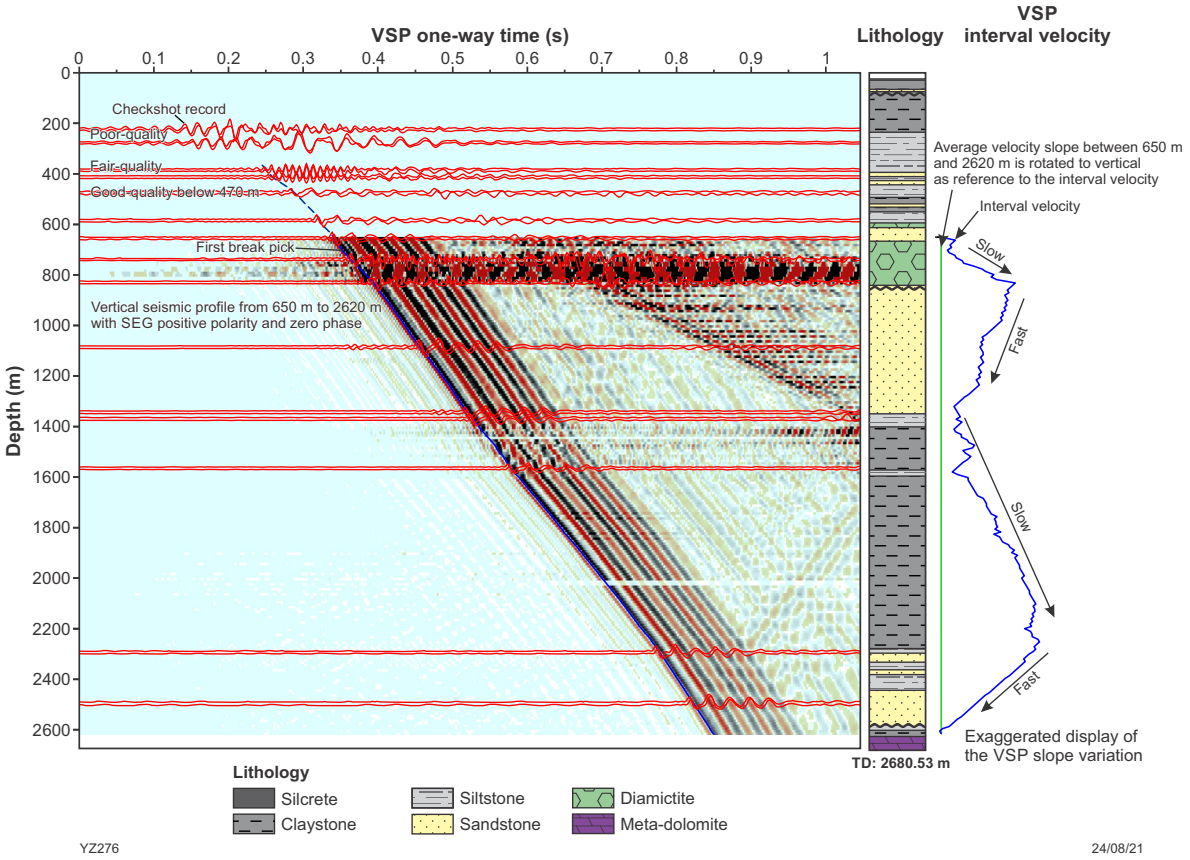

Figure 10. VSP and checkshot records. First break picks were provided by Hiseis. The interval velocity is derived from the VSP slope variation and shows a consistency with lithological packages: fast velocity predominantly in sandstone and slow in mudstone-dominated diamictite and claystone

The first arrivals measured inside the PQ casing are mostly good-quality due to the small annulus between the borewall and casing, except for the upper- and lower-most parts of the well (727–825 m and 1400–1610 m) where there is a lack of hard-coupling with rock formations. Between 650 and 727 m the data show a good quality with OWT between 0.35 and 0.4 s despite being logged through two sets of casing (PQ and SQ casings).

Checkshot data were collected (wiggle lines in Figure 10) when lowering the logging tool, prior to pulling up for the VSP measurements. The checkshot points were selected at the boundaries of major lithological zones to measure the OWT as anchor points for well calibration with the seismic line. The checkshot data is good quality below 450 m, showing that the first break is consistent with the VSP at each trace record. The data is of reasonable quality at 380 and 420 m, but it becomes difficult to interpret at 220 and 280 m.

Quality control of velocity data

Based on the VSP, checkshot and sonic data, the velocities in the shallow sections are much slower than normal rock formations:

- the average velocity within the upper 650 m is calculated at 1895 m/s via the arrival time of 343 ms from VSP measurement (Figure 10 and Step 1 in Figure 11)
- the top reliable checkshot at 470 m shows an arrival time of 290 ms (Fig. 10), yielding an average velocity of 1621 m/s
- the VSP and sonic data can lead to an interval velocity of 986 m/s with an arrival time of 213 ms for the top 210 m (Steps 1–3 in Figure 11).

These velocity values are unrealistically slow, especially the 986 m/s, which is slower than water (1480 m/s) and only higher than air (343 m/s) within common mediums of wave propagation. In general, such low velocity is only applicable within the shallowest part of the weathering layer but rarely exists for thick layers, such as the top 210 m in Barnicarndy 1 (R Taylor, 2020, written comm.) In addition, the VSP recorded 0.85 s one-way travel time (1.7 s TWT) at 2620 m near the bottom of the Paleozoic sedimentary package (Fig. 10). Such a measurement is about 0.3 s deeper than the reflective package in the Barnicarndy Graben on the Kidson seismic profile. This inconsistency, in conjunction with the unrealistically slow velocity for the shallow section, indicates that a systematic delay exists in receiving the VSP and checkshot signal. Those absolute time–depth pairs from VSP can cause the erroneous velocity and poor well-seismic calibration. However, the systematic time delays should be a constant value for all the measurement points. Thus the delays would be cancelled out during the calculation of the interval velocity ($\Delta Z/\Delta t$; ΔZ is the depth interval between any two geophones, and Δt is the travel time difference measured from those two geophones; red line in Figure 8).

The VSP interval velocity calculation can avoid the constant time delay. However, the velocity may be affected by acquisition and processing errors and inaccurate

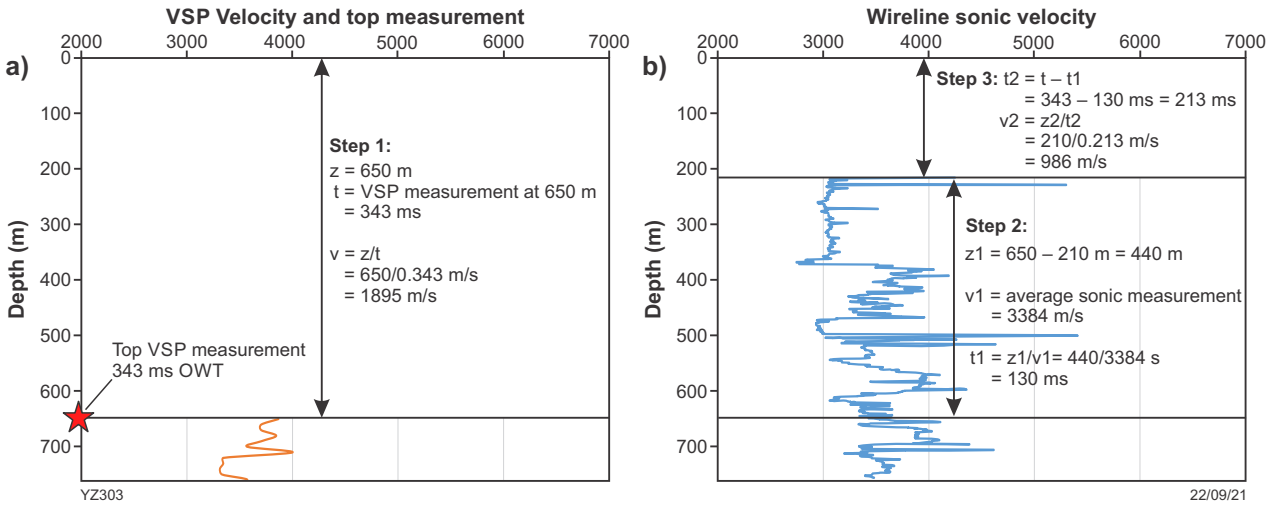

Figure 11. Velocity calculation in the upper-most unlogged section (0–210 m): a) VSP top measurement at 650 m and interval velocity; b) sonic velocity below 210 m

interpretation of the first break. For example, an error of 1 ms in the first break interpretation between two measuring points 10 m apart could lead to over 1000 m/s difference in the calculated velocity. Thus, the original first break interpretation of the Barnicarndy 1 VSP has been smoothed at individual points (Table 2). The instrumental and/or interpretational errors can also be greatly reduced after averaging the velocity for intervals over 100 m to create a smoothed velocity curve.

After despiking the interval velocity at individual points, the results can be used to compare with lithological packages in Barnicarndy 1. The prominent arrivals on the profile appear to be a straight line from 650 to 2620 m (Fig. 10). However, there are subtle variations on its slope that indicate the rock velocity changes throughout the borehole. To manifest the velocity variations, the slope is processed with a few steps: the picks at the top and bottom of measurements are connected as a straight line to represent the average velocity between the points; then the straight line for the average velocity and first break picks for the interval velocity are bundled and rotated to the vertical position; finally the line representing interval velocity is horizontally exaggerated for qualitative analysis. When referenced to the vertical line, the relative interval velocity can be indicated by its slope (dark blue line in Figure 10): slow to the right and fast to the left. The distinct inflections along the curve are fairly consistent with the lithology variations, showing fast velocity predominantly in the sandstones and slow velocities in the mudstones.

The VSP interval velocity also needs to be compared with the sonic velocity to check if they reasonably match. The VSP measures one-way travel time at an intermediate scale between the vibroseis source and the downhole geophone sensors within the borehole to enable calibration with the seismic survey, compared to the closely spaced measurements derived from the sonic wireline logs (Fig. 7). The sonic compressional velocity is calculated from the inverse of sonic slowness after amalgamation of three logging runs and petrophysical correction (blue line in Figure 8; Walker Petrophysics, 2020). Between 650 and 2620 m, the VSP velocity is mostly slower than the velocity derived from the wireline sonic data with an overall drift of about 3.5% between them (Table 3). The variation between them is considered as reasonable, given the different volumes of rock in measurement and different sources and frequencies of the instruments.

Noticeably, the velocity differences between the VSP and wireline sonic log are greater in the porous sandstone than the claystone (Fig. 8; Table 3). This is probably caused by drilling mud invasion into the high porosity intervals, which is measured as a higher velocity by the sonic tool (Fig. 7). As a result, the VSP velocities are considered more robust than the velocities derived from the sonic log, especially for its travel time difference (Δt; 510 ms OWT) between the top (650 m) and bottom (2620 m) measurements. Therefore, the VSP data is used to correlate between the synthetic seismograms and the Kidson seismic survey.

In summary, the quality control of the velocity data has found that the VSP had instrumental delay in the acquisition, based on unrealistically slow velocity in the uppermost 210 m and poor seismic correlation. However, after cancelling out the time delay and despiking erroneous data at individual points, the VSP interval velocity was consistent with the lithological packages and showed reasonable matches with sonic velocity, given consideration of the mud-cake effect.

Uncertainty analysis

Seismic interpretation difficulty

Wildcat exploration wells in the Canning Basin (e.g. Ungani 1 in Buru Energy Limited, 2013; Asgard 1 in Buru Energy Limited, 2014) often have considerable mismatches between predicted and actual formation tops due to sparse well data and widely spaced seismic grids. This was also the case for Barnicarndy 1 where no wells had been drilled in the graben below the Permian, and the formation predictions were based entirely on seismic characteristics and expected to have discrepancies on the formation picks.

Three major seismic horizons, the Base Mesozoic, Base Permian and Top basement, were interpreted for pre-drill planning (Fig. 3). These major picks, along with the Ordovician to Silurian horizons between the Base Permian and Top basement, carried inherent uncertainties and were expected to be shallower or deeper in TWT than their actual reflectors due to the lack of data to tie to the interpretation. The interpretation difficulty was exacerbated for the Base Permian and Top basement horizons, which could easily have one wavelength (equivalent to 100–150 m) difference compared to the actual boundary encountered in the well. The Base Mesozoic was also subject to erroneous interpretation, as its existence had not yet been confirmed. However, any uncertainties or mis-picks in interpreting shallow horizons does not accumulate or increase the discrepancy on deeper ones, as the horizons are picked individually and independent from each other.

Velocity beyond range

With the quality control discussed above, the VSP and sonic velocity are found to be reasonably consistent with each other and they match the lithological packages. This consistency verifies that the velocity of the Barnicarndy 1 stratigraphy below 210 m is unexpectedly fast and does not follow the trend observed from offset wells (Fig. 9). The sonic log shows that the velocities start off at 3000 m/s at 210 m, 3500 m/s at 450 m and 4200 m/s at 855 m in the shallow diamictite and sandstone (Fig. 9). It is possible that the high velocity extends upwards from 210 to 96 m just immediately below the weathering layer, despite the lack of velocity measurement. Below 210 m, the velocities are approximately 500–1000 m/s faster than the offset wells at equivalent depths. The occurrence of anomalous velocities in the shallow clastic packages may indicate that the Permian section in the Barnicarndy Graben might have been more deeply buried and a large amount of overlying section has been eroded after the Permian. This corroborates

Table 2. Example of the effect of a subtle revision on the Barnicarndy 1 VSP OWT from the first break interpretation. Note the original pick at 1109.8 m (469.34 ms) causes an erroneous velocity disparity (2747 vs 6842 m/s, in italics) for the interval above and below. A 1 ms revision (468.34 ms) at this individual depth can move both velocities into the normal range without affecting overall time–depth relation

Depth (m)	*Original OWT (ms)*	*Calculated interval velocity (m/s)*	*Revised OWT (ms)*	*Recalculated interval velocity (m/s)*
1079.97	460.3		460.3	
		3704		3704
1089.81	463		463	
		3700		3700
1099.8	465.7		465.7	
		2747		*3788*
1109.8	469.34		468.34	
		6842		*4061*
1119.79	470.8		470.8	
		3568		3568
1129.78	473.6		473.6	
		4016		4016
1139.78	476.09		476.09	

Table 3. Velocity difference of various lithologies in Barnicarndy 1 between VSP and wireline sonic data

Depth interval	*Lithology*	*VSP interval velocity (m/s)*	*Wireline sonic velocity (m/s)*	*Velocity difference*
650–726	Silty sandstone and diamictite	3640	3686	1.26%
726–828	Mud-dominated diamictite	3180	3258	2.47%
828–1100	Sandstone	3892	4205	8.04%
1100–1340	Sandstone	4103	4269	4.03%
1620–2000	Claystone	3589	3694	2.92%
2000–2270	Claystone	3792	3895	2.72%
2270–2585	Tight sandstone	4555	4583	0.63%

vitrinite and vitrinite equivalence determinations by Ranasinghe and Crosdale (2020), which put the oil window as shallow as 610 m.

The high velocity below the weathering layer has a cumulative effect on the depth prognosis for both the shallow and deep parts of the well, compared to the uncertainty for individual horizon picks from the seismic interpretation. The velocity impact on the deep section is illustrated here using the comparison between Barnicarndy 1 and Frankenstein 1, which has the highest velocity among the offset wells. The interval velocities (470–855 m) in Barnicarndy 1 and Frankenstein 1 are calculated at 3545 m/s and 2990 m/s, respectively. This high velocity in the 388 m thick diamictite interval in Barnicarndy 1 reduces the seismic TWT by about 40 ms, which produced about 100 m difference in the depth prediction at the Top basement horizon. Similarly, the interval velocity in the sandstone (855–1345 m) directly beneath the Permian is also much higher than Frankenstein 1 and other offset wells (Fig. 9). The high velocity in this interval exacerbated the depth prognosis at the Top basement. Due to the thick package of claystone between 1600 and 2270 m, the interval velocity slightly slows (reverses) back to less than 4000 m/s, which is comparable with the velocity at similar depths in the offset wells (Fig. 9). This relatively low velocity slightly cancels out the depth difference caused by the high velocity in the shallow section.

Out-of-plane reflection

Out-of-plane reflection can be intuitively likened to a visual phenomenon of an observer above water that sees the apparent position of a fish shallower than its actual position, due to refraction and reflection in the water. In seismic reflection, two-dimensional surveys in the acquisition and processing have an underlying assumption that the data provide a vertical image of the subsurface structure within the plane of the seismic acquisition. This normally is the case when the strata are horizontally layered, which is typical in basin-filled sedimentary rocks, as seismic waves travelling in the vertical plane will be reflected back via the shortest route. However, the reflection plane is not always vertical, especially in crystalline and metamorphic basement. This is because the seismic wave originating at a specific source does not propagate in one particular direction but expands in a series of spherical wavefronts, and reflects back from all different directions. In the case of irregular geometry of the subsurface, the out-of-plane reflection can arrive at geophones faster than the vertical in-plane, and cause ambiguities for seismic processing and interpretation (Fig. 12).

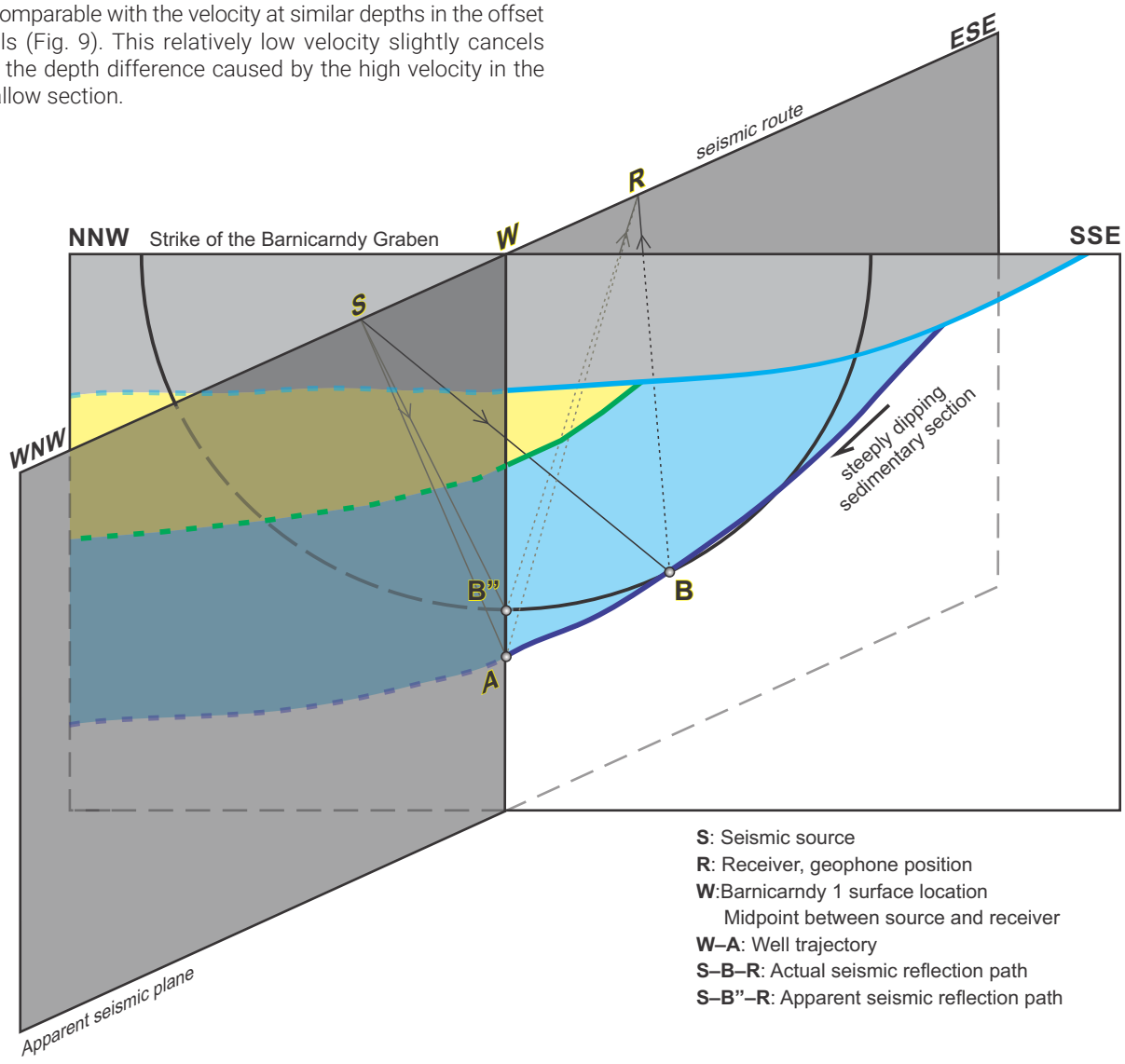

Figure 12. Schematic diagrams showing the out-of-plane effect on seismic reflection that likely occurred within the Barnicarndy Graben (modified after Drummond at al., 2004)

This out-of-plane scenario may also be the case for Barnicarndy 1 due to the steeply dipping strata on the margins of the graben (Fig. 12). Based on gravity and magnetic images and proximity to basement outcrops about 13 km south of the line, Barnicarndy 1 is interpreted to be near the south-southeast end of the graben. The sedimentary succession in the embayment is interpreted to be steeply dipping down towards the north-northwest (Figs 12, 13a) and may be faulted resulting in significant vertical displacement between the outcrop and deeply buried areas, such as seen on the Ryan Shelf to the east of the Kidson Sub-basin (Fig. 13b). However, due to localized undulation, the dip of the strata near the well is difficult to quantify. The pre-Permian stratigraphy often has a steeper dip than the overlying Permian at the basin margins, as seen on as the eastern and western margins of the Kidson Sub-basin on the Kidson seismic survey (Fig. 13b; Southby et al, 2019; Zhan and Haines, 2021).

For a flat-lying basement underlying homogeneous sedimentary succession, the in-plane reflection will arrive faster than out-of-plane reflections, which have a longer travel time and will be attenuated or even eliminated during seismic processing. However, the reflection path will be different for steeply dipping strata. The out-of-plane effect on energy recorded along the Kidson seismic survey is illustrated on a 3D schematic diagram with two intersected planes (Fig. 12; modified after Drummond at al., 2004): west-northwest to east-southeast plane as the seismic route, and north-northwest to south-southeast plane along the strike of the Barnicarndy Graben showing the slope in the south-southeast margin. At the mid-point (W), the in-plane seismic energy will travel from the source (S), reflect off the Top basement (in-plane A vs out-of-plane B), and arrive to the geophone (R) with a total travel time T_{SAR} and $T_{SBR,}$ which will be corrected to vertical two-way travel time $T0_{SAR}$ and $T0_{SBR}$ after normal moveout, respectively. The semi-circle represents a hemispherical surface of depth points with the same travel time as $T0_{SBR}$. In the case of a steeply dipping basement (bold blue line), the out-of-plane reflected wave will arrive earlier than the in-plane wave ($T0_{SBR}$<$T0_{SAR}$), and the in-plane reflection will be attenuated in the processing or lead to out-of-phase stack when combined with the near-plane reflection energy.

The basement is interpreted to have significant dip near the south-southeast end of the Barnicarndy Graben as discussed above. It is likely that the Kidson seismic survey does not reflect entirely from within the vertical plane of the survey line, but images the shallower out-of-plane basement structures to the south of the survey than the in-plane section where the well is drilled.

Discussion

The absolute time–depth pairs from the original VSP data show that the basement at 2585 m corresponds to 1.7 s TWT, which is about 0.3 s below the seismic reflective package responding to the Paleozoic sedimentary rocks of the Barnicarndy Graben. This anomalous calibration is probably caused by instrumental delays in the VSP acquisition. After removing the uncertain but unchanged delays, the interval velocity from the VSP is consistent with the lithological package and reasonably matches the sonic velocity. This VSP interval velocity provides a relative time–depth relation that the seismic energy takes 510 ms OWT to travel between the top (650 m) and the base (2620 m) measured VSP points (Fig. 10). The relative time–depth also incorporates good-quality checkshots between 470 m and 650 m. The integrated relative pairs are then vertically shifted, without squeezing or stretching, to maintain the interval velocity by certain amounts of time in compensating for the uncertainties from the impact of systematic VSP delay.

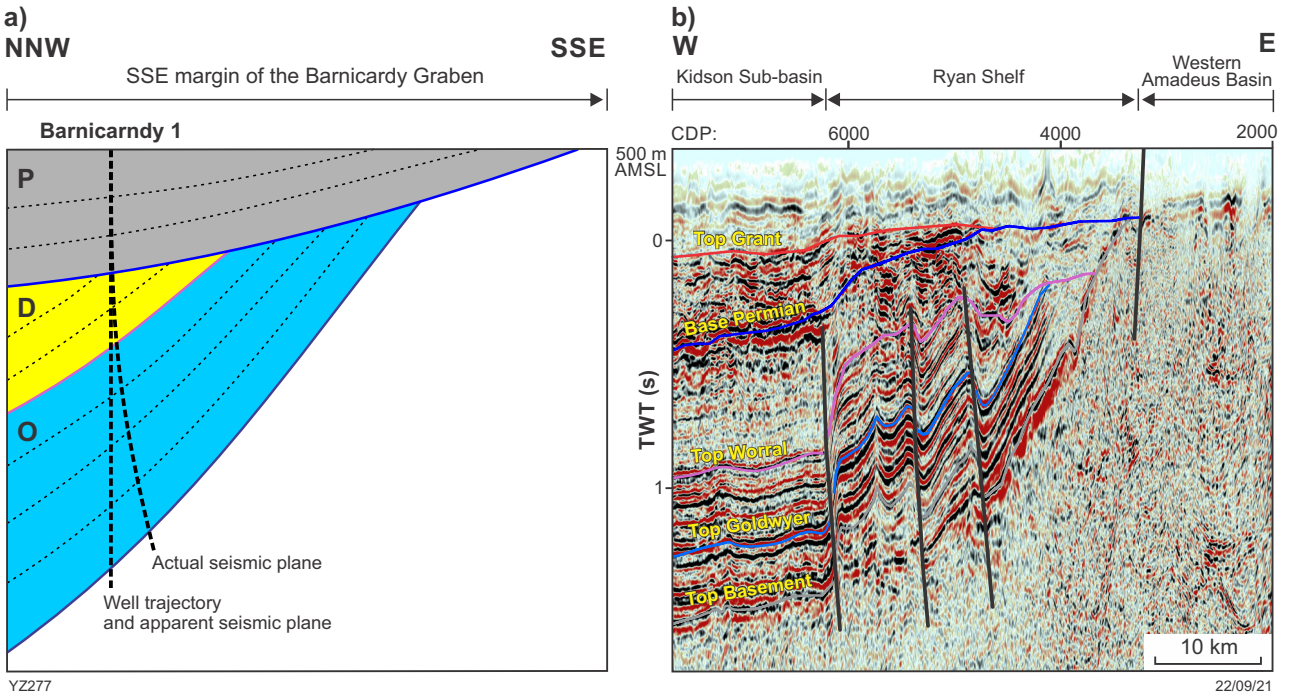

Figure 13. Geometries of the basin margins: a) conceptual model with steeply dipping strata in the south-southeast margin of the Barnicarndy Graben; b) similar geometry with fault displacements in the eastern margin of the Kidson Sub-basin

Three segments of the Barnicarndy 1 sonic compressional velocity and formation density logs were merged and corrected (Walker Petrophysics, 2020) as the basic input to compute acoustic impedance to produce the synthetic seismogram. Shear wave velocity is not incorporated for synthetic modelling, as the fluid response and amplitude vs offset effects are not within the scope of the study. For synthetic correlation purposes, the seismic datum is placed at ground level, which at the Barnicarndy 1 well location is calculated to be 194 ms below the start time (400 ms above MSL) based on the final datum (500 m above MSL), surface elevation (258 m above MSL) and replacement velocity (2500 m/s). Different time shifts were applied to VSP time–depth pairs in order to find the optimal fit with the seismic data. Despite the time shifts, the synthetics still did not match with the seismic for the entire well trajectory, no matter what wavelet frequencies or phases were applied (Figs 14, 15). Possible reasons for the poor correlation include the mud invasion affecting the wireline log response within porous sandstone intervals, different logging tools used in Run 3 compared to Run 1 and Run 2, environmental corrections and out-of-plane seismic reflection. Nevertheless, three options of time shift (215, 96, 270 ms) seem to have geologically meaningful correlations between the synthetic and real seismic trace for parts of the well.

215 ms shift

The VSP shift of 215 ms gives the best tie to the seismic interpretation, as both the stratigraphy and wireline logs are a good match with the seismic profile for the upper half of the well from 210 to 1500 m. Beneath 1500 m the synthetic reflectors are deeper than the seismic trace, therefore the correlation coefficient, which represents the similarity between the synthetic and seismic, is computed separately for the upper half (210–1500 m; r1 in Figure 15) along with the entire logging path (210–2685 m; r2). Various wavelets of different frequencies and phases are used to attain the best possible correlation between the synthetic and seismic section, showing that a wavelet with 32 Hz, minimum phase and SEG positive polarity presents the highest reflection correlation coefficient for both r1 and r2 (Fig. 15).

After the 215 ms time shift (Fig. 16), the uppermost claystone in the Permian at 210 m points to a relatively strong reflector where it was originally picked as Base Mesozoic (0.18 s). The Permian (210–855 m) section correlates to the upper strong but chaotic zone with the base matching the previous TWT interpretation at ~0.6 s. The underlying sandstone package (855–1345 m) coincides with a thick zone of weak-amplitude reflectors from ~0.6 to 0.83 s. The change of velocity and density in the middle of the sandstone package at 1070 m induces a relatively strong reflection on the synthetic trace and calibrates to a long-wavelength, but discontinuous, peak reflector at 0.71 ms in the middle of the bland zone on the seismic profile.

However, the section below 1392 m appears to have inadequate correlation between the synthetic and seismic traces. The mismatches are evident in the upper part of the claystone below 1392 m (Fig. 16). Within this interval, the lithology, wireline logs and synthetic seismogram do not suggest much variation, whereas the seismic section shows a set of high-amplitude reflectors indicating variable petrophysicial properties. The reason is unclear for the mismatch in this part of the claystone. Perhaps the seismic reflection is interfered by multiples reflected within the siltstone (1345–1392 m) above the claystone. The discrepancy between the synthetic and seismic also occurs in the lower sandstone and basement below 2270 m, which requires an additional ~55 ms shift in order to match this interval separately (see the insert in Figure 16 for the correlation in the lower part of the well). This mismatch is interpreted to be caused by out-of-plane reflections from the upwardly steep dipping basement south of the seismic survey (2455 m). The ~55 ms extra shift related to the out-of-plane reflection accounts for the ~130 m difference between the prognosed and actual depth to the Top basement.

Based on the synthetic seismic correlation, the original seismic TWT interpretation prior to the drilling is mostly consistent with the actual formation boundaries. The shallow depth prognosis is mainly related to the velocities in the upper half of the well above 1392 m. The velocities are about 500–1000 m/s higher than the offset wells (Fig. 8). The fast velocities in the shallow formations aggregate the depth difference in the deeper section (Table 4), such as 695 m vs 855 m at Base Permian, 1050 m vs 1345 m at the base of the thick sandstone. The prognosis error in basement depth is associated with both velocity and out-of-plane reflection issues. The interpretation of Top basement at the sharp strong amplitude about 1.22 s below MSL (2200 ± 275 m in prognosis; Table 4) pinpoints to 2455 m on the seismic plane based on the seismic calibration. This shows a 255 m difference caused by the fast velocity in the Permian diamictite and the underlying sandstone. The rest of the difference (about 130 m) is interpreted to relate to the out-of-plane seismic reflection from south of the drilling site, based on the mismatch in the bottom part of the well (see the insert in Figure 16).

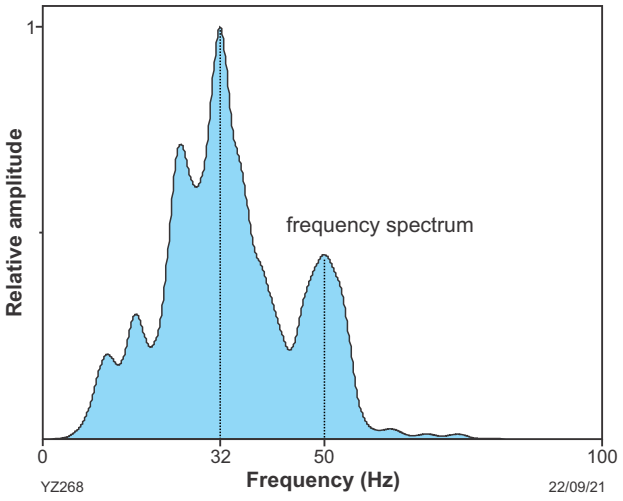

Figure 14. Frequency spectrum analysis, showing 32 Hz as the dominant frequency of the key interval of the seismic trace from the Kidson seismic survey near Barnicarndy 1

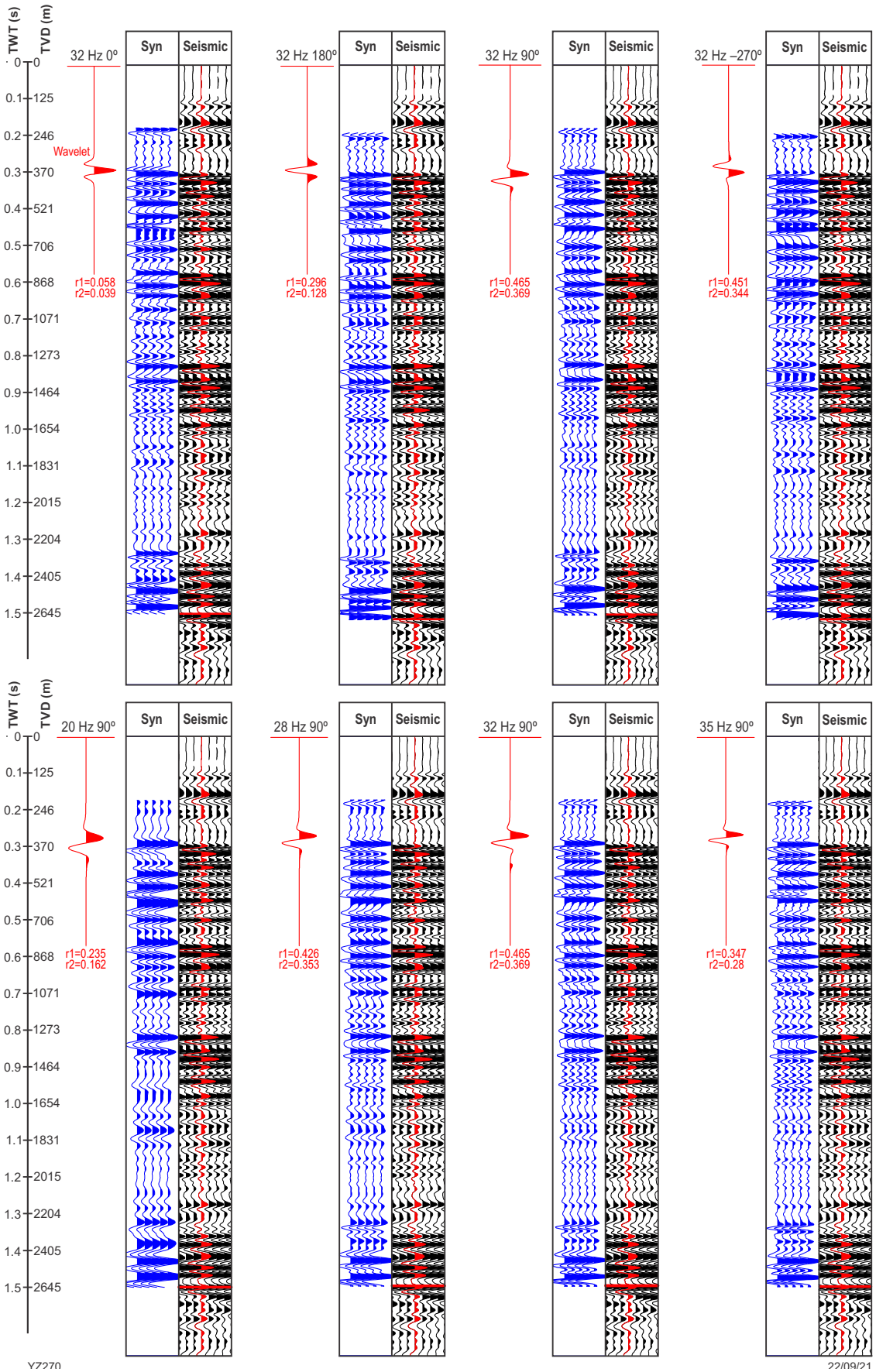

Figure 15. Comparison of synthetic and seismic correlations with various wavelet candidates of different frequencies and phases. The correlation coefficients (r1 and r2) are computed for the upper part from 210 to 1500 m and the entire logging path from 210 to 2680.5 m, respectively. Both coefficients show that the wavelet of 32 Hz and 90 degrees generate the optimal synthetic correlation. After excluding the mismatch in the lower part of the well, the upper part generally has a better correlation coefficient than the entire logging path

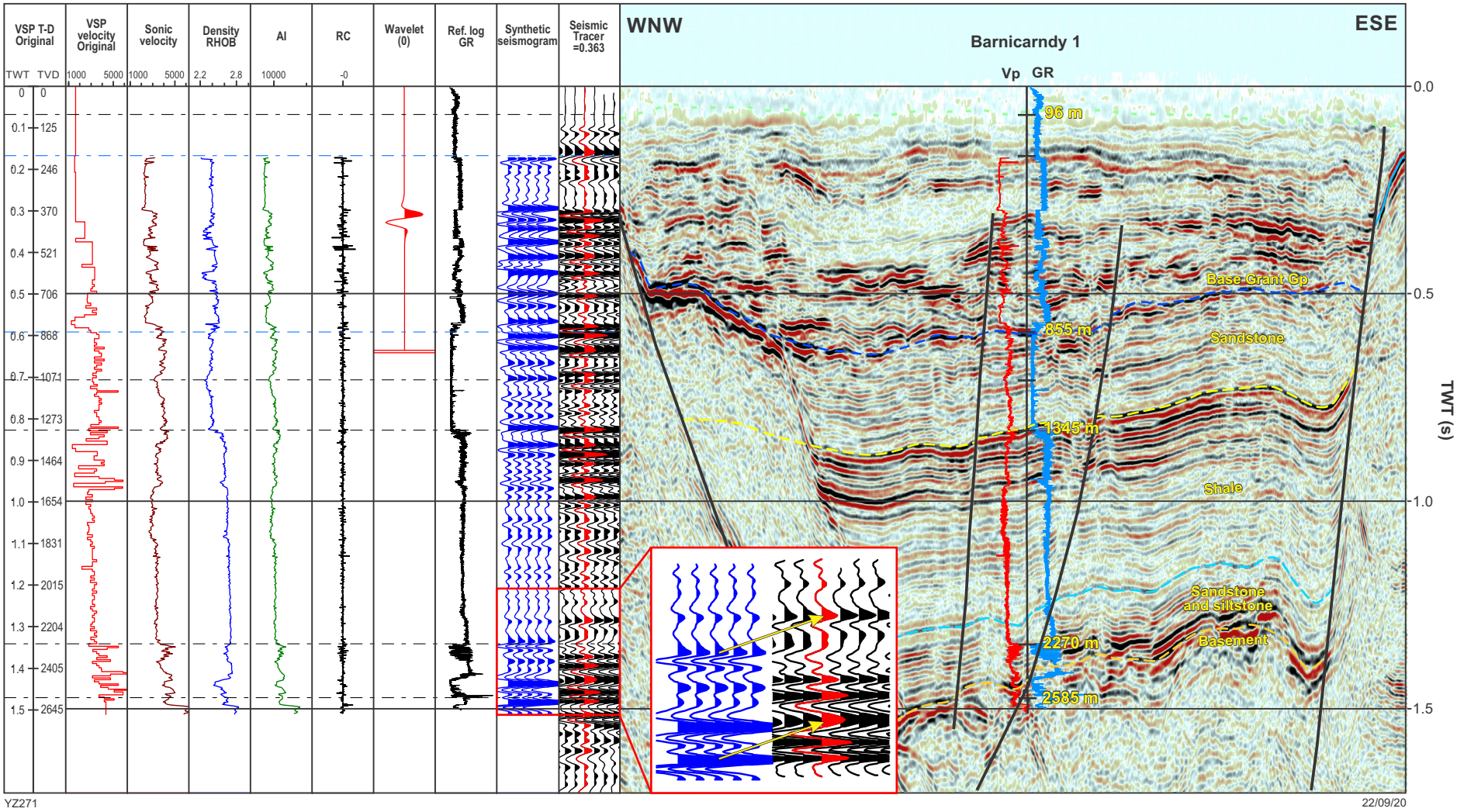

Figure 16. Synthetic seismic correlation after shifting Barnicarndy 1 VSP time–depth pairs upwards by 215 ms. The bottom part of the well shows a mismatch and requires an additional 55 ms shift for correlation (see yellow arrows in the enlarged box)

Table 4. Impacts of the velocity anomalies and out-of-plane issues in the prognosis of Barnicarndy 1

TWT (ms) datum (0 ms) at surface	*TWT (ms) datum (0 ms) at MSL*	*Depth prognosis (m)*	*Depth on corrected VSP after synthetic correlation (m)*	*Depth difference due to high velocity (m)*	*Depth difference caused by out-of-plane reflection (m)*	*Comments*
180	–20	210 ± 50	210	0	N/A	*Permian intra-formational boundary
600	400	695 ± 90	855	160	N/A	**Base Grant Group
840	640	1050 ± 150	1345	≤295	Unknown	Top claystone
1420	1220	2200 ± 275	2455	255	130	Top basement

NOTES: * This seismic horizon was interpreted pre-drill as Base Mesozoic; based on Barnicarndy 1 palynology data and HyLogger spectral analysis, it appears to be an intra-formational boundary at 210 m between claystone and sandstone within the Permian. The weathering layer probably has a thickness of ~96 m, which does not show a reflection event on the seismic section at 0.06 s

** The seismic horizon was interpreted Based Permian Grant Group, which has been re-interpreted to reach into Carboniferous in the bottom part of the Group (Backhouse and Mory, 2020)

96 ms shift

The 96 ms shift (Fig. 17) enables a good synthetic–seismic match from the middle of the sandstone package (1070 m at 0.82 ms) to a lower part of the claystone (1950 m at 1285 ms). With this shift, the overall average velocity curve becomes comparable to that of offset wells. The pre-drill TWT interpretation for the Top basement at 1.22 s below MSL also correlates to 2210 m, which matches with the prognosis. However, this shift leads to a relatively poor correlation between synthetic and seismic trace within the Permian section (Fig. 17). This is evident in the silty part of the section between ~260 and ~360 m (~0.3 to ~0.4 s), which is a bland zone on the synthetic profile but highly reflective on the seismic section. Another difficulty lies in the lower part of the sandstone and basement with a mismatch about 170 ms (375 m). This requires a significant amount of the out-of-plane effect to solely account for the mismatch. The synthetic mismatch in the shallow (0.3 – 0.4 s) and the 375 m out-of-plane impact are considered not as plausible as the correlation after the 215 ms shift.

270 ms shift

The 215 and 96 ms time shifts focus on the synthetic to seismic correlation of the Permian (210–855 m) and part of the underlying sandstone and claystone (1070 and 1950 m), respectively. Both lead to synthetic to seismic correlation discrepancies for the lower part of the sandstone and basement. In order to correlate this part of the well, a 270 ms upwards shift of the synthetic seismogram is required to enable a good match from the lower part of the claystone to the basement (Fig. 18). This suggests that the seismic reflector at the Top basement has a high amplitude at 1.42 s below ground level, where it was originally interpreted. The difficulty with this amount of shift is the lack of synthetic to seismic consistency above the lower claystone from 210 to 1950 m, and results in major lithological boundaries to calibrate with indistinct reflectors on the seismic section, such as the top claystone at 1392 m in the middle of a bland zone at 0.78 s (Fig. 18). Due to the significant mismatch in the upper part of the well, the 270 ms shift is not considered an optimal option, but it indicates that the true reflectors of the sandstone and basement are relatively shallower on the seismic plane than the in-plane drilling location.

Conclusions

The post-drill analysis of Barnicarndy 1 has identified discrepancies in several data types, including mismatches between original VSP time–depth pairs and the seismic profile, poor correlation between the synthetic and seismic trace, as well as velocity differences between VSP and sonic logs. These inconsistencies have led to uncertainties in the post-drill interpretation and prompted detailed analyses using different types of datasets.

The interval velocity calculated from the VSP data is reasonably consistent with the wireline sonic data. The overall variation of about 3.5% is probably related to the different sources and frequencies of the instruments. Compared with the VSP seismic methodology, the high-frequency sonic tool has a limited depth of investigation, so the measurement was compromised to a certain extent by drilling mud invasion into the porous sandstones. However, the uppermost 210 m sediment package is estimated to have an average velocity of less than 1000 m/s, based on the absolute VSP time–depth and wireline logs. Such velocity is unrealistically slow and probably caused by a systematic time delay in the acquisition of the VSP data. Moreover, the absolute VSP data calibrate the Top basement into a non-reflective zone about 300 ms below the sedimentary package with poor correlation between the synthetic and seismic section. These difficulties produce low confidence to use the absolute time–depth pairs of the VSP to correlate with the seismic section.

Given the VSP is consistent with lithological packages and reasonably matches the sonic velocity, this study uses the VSP relative time–depth function (interval velocity) to calibrate the synthetic with the seismic section. The relative time–depth relation is manually shifted upwards, without stretching or squeezing, to preserve the interval velocity and to counteract the possible time delay in the VSP data. Three options of time shift are considered having meaningful correlation between the synthetic and seismic traces.

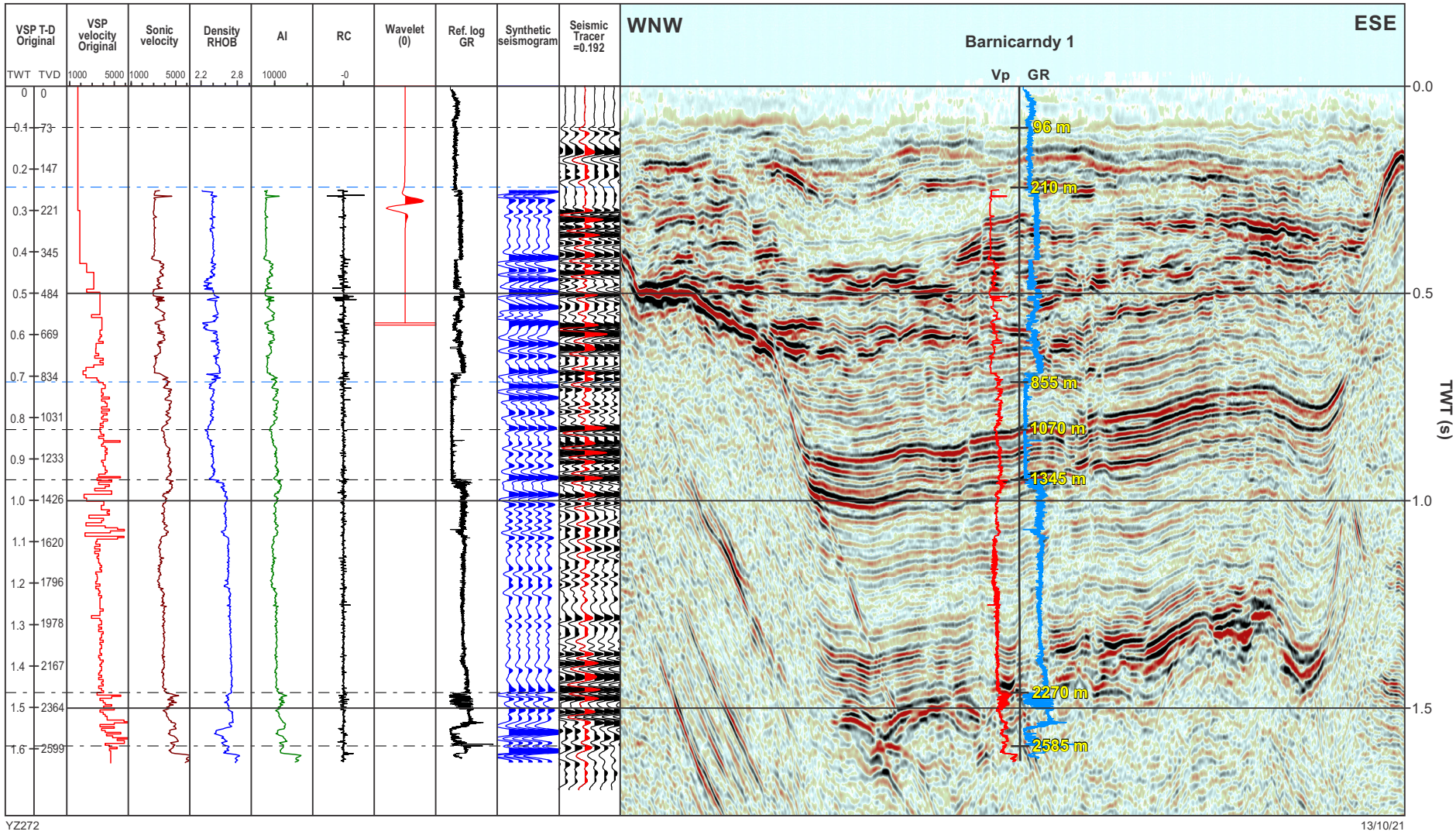

Figure 17. Synthetic seismic correlation after shifting Barnicarndy 1 VSP time–depth pairs upwards by 96 ms

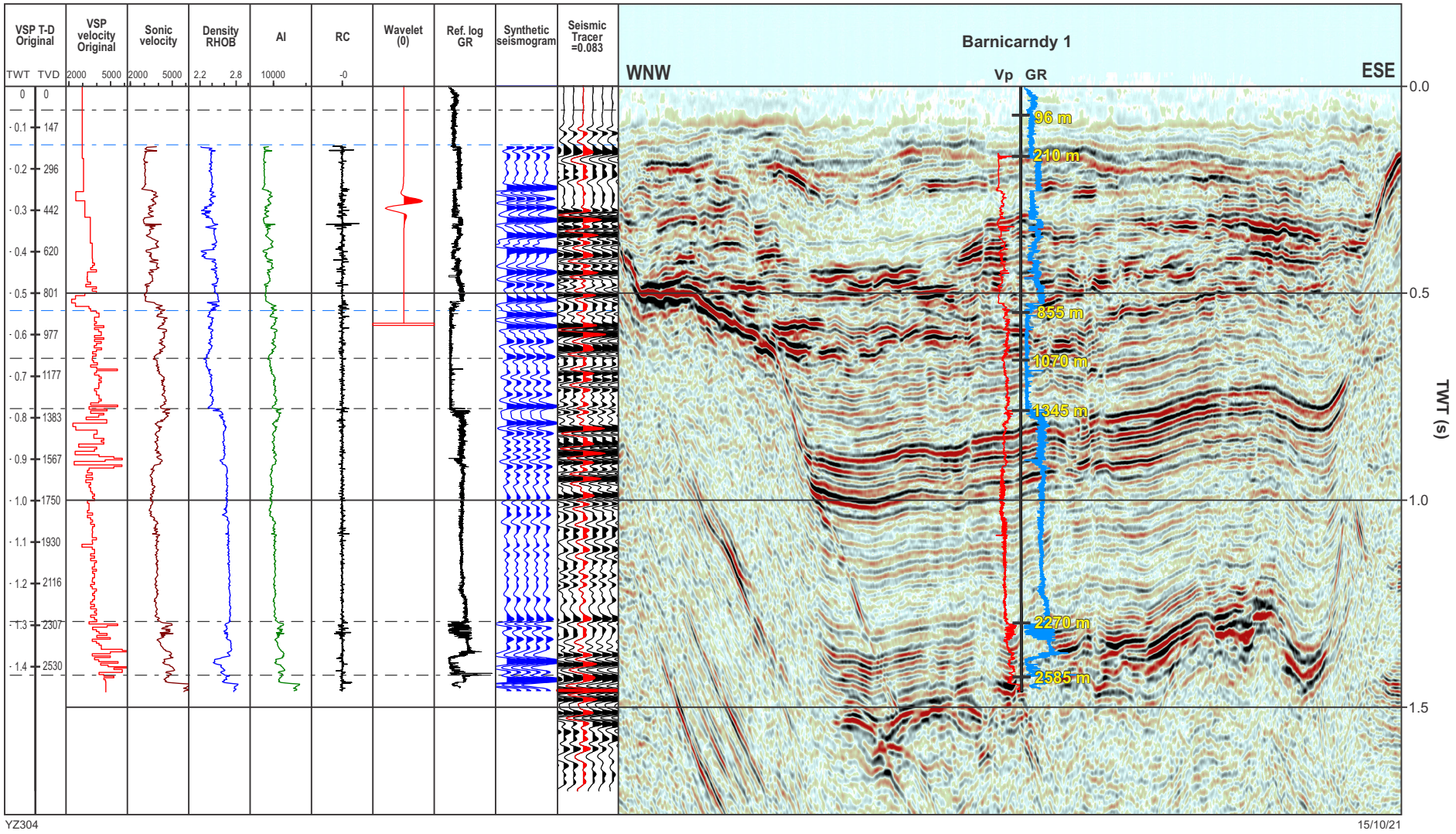

Figure 18. Synthetic seismic correlation after shifting Barnicarndy 1 VSP time–depth pairs upwards by 270 ms

The 215 ms upwards shift is evaluated as the optimal solution that enables a better synthetic correlation with the seismic section. However, it is still difficult to reconcile two sections of the well: the upper portion of the claystone (1392–1600 m), possibly caused by interference of reflection multiples, and the lower-most section below 2270 m from sandstone and basement, likely due to out-of-plane reflection.

With a 215 ms upwards shift, the original seismic interpretation for the major boundaries is mostly consistent in TWT with what was penetrated in Barnicarndy 1. The depth errors of prognosis, such as 2200 ± 275 m in prediction compared to 2585 m in actual intersection of the Top basement, were largely caused by the high velocity in Barnicarndy 1 in the shallow sections. The velocity starts off at 3000 m/s at 210 m (~48 m above MSL) and increases with depth in the Permian and underlying sandstone between 855 and 1345 m. The velocities in these sections are approximately 500 to 1000 m/s faster than other wells at equivalent depths. The velocity reverses back to a normal range in the deep claystone with an average value of 3900 m/s at 2000 m, which slightly cancels out the depth calculated to Top basement. However, the basement reflections on the Kidson seismic survey are also impacted by the out-of-plane reflections resulting in a shallower image of the basement unconformity. Based on the synthetic correlation for the deep section this impact is quantified to result in an extra 130 m difference at the Top basement between the in-plane drilling and the out-of-plane seismic section. The high velocities of the Permian strata and underlying sandstone may indicate that the Barnicarndy Graben had previously been buried much deeper than seen present day and a large amount of overlying sedimentary section has been eroded.

Acknowledgement

The author thanks Randall Taylor (Taylor Exploration Consulting, and former chief geophysicist at Origin Energy) and Ikae Brown (Senior Geophysicist at Petroleum Compliance of the Department of Mines Industry Regulation and Safety) for their constructive comments and suggestions.

References

Alavi, SN 2013, Structure, stratigraphy, and petroleum prospectivity of the Waukarlycarly Embayment, Canning Basin, Western Australia: Geological Survey of Western Australia, Record 2013/10, 32p.

Allen, KA, Eder, J and Tipps, RD 1971, Final report Canning Basin Anketell seismic survey (Projects 277 and 283); West Australian Petroleum Pty Ltd: Geological Survey of Western Australia, Statutory petroleum exploration report S614 A1, 152p.

Backhouse, J and Mory, AJ 2020, Mid-Carboniferous – Lower Permian palynology and stratigraphy, Canning Basin, Western Australia: Geological Survey of Western Australia, Report 207, 133p.

Buru Energy Limited 2013, Ungani and Ungani 1ST1 well completion report volume 2 – Derivative data: Exploration permit EP 391 Canning Basin, Western Australia: Geological Survey of Western Australia, Statutory petroleum exploration report W21513 A3, 153p.

Buru Energy Limited 2014, Asgard 1 well completion report volume 2 – Derivative data: Exploration permit EP 371 Canning Basin, Western Australia: Geological Survey of Western Australia, Statutory petroleum exploration report W21543 A2, 308p.

Carr, LK, Edwards, DS, Southby, C, Henson, P, Haines, P, Normore, L, Zhan, A, Brooks, D, MacFarlane, S, Boreham, CJ, Grosjean, E, Mory, AJ, Wang, L and Gunning, M-E 2020, Kidson Sub-basin seismic survey and Waukarlycarly 1 stratigraphic well: an acquisition program for evaluating Canning Basin petroleum systems, *in* Exploring for the Future: Extended Abstracts *edited by* K Czarnota, S Abbott, M Haynes, N Kositcin, A Ray and E Slatter: Geoscience Australia, Canberra, p. 4., doi:10.11636/134073.

Command Petroleum NL 1989, Frankenstein-1, Canning Basin, well completion report, EP 232: Command Petroleum NL: Geological Survey of Western Australia, Statutory petroleum exploration report S3417 A2V1, 90p.

Dix, CH 1955, Seismic velocities from surface measurements: Geophysics, v. 20, no. 1, p. 68–86.

Drummond, BJ, Hobbs, RW and Goleby, BR 2004, The effects of out-of-plane seismic energy on reflections in crustal-scale 2D seismic sections: Tectonophysics, v. 388, no. 1–4, p. 213–224.

Forman, DJ and Wales, DW 1981, Geological evolution of the Canning Basin, Western Australia: Bureau of Mineral Resources, Geology and Geophysics, Bulletin 210, 91p.

Fraser, AR 1976, Gravity provinces and their nomenclature: BMR Journal of Australian Geology and Geophysics, v. 1, p. 350–352.

Frogtech Geoscience 2017, Canning Basin SEEBASE study and GIS data package: Geological Survey of Western Australia, Report 182, 297p.

Geological Survey of Western Australia 2017, 1:500 000 tectonic units of Western Australia, 2017: Geological Survey of Western Australia, <www.dmirs.wa.gov.au/ebookshop>.

Geological Survey of Western Australia 2020, Gravity anomaly grid (400 m) of Western Australia (2020 – version 1): Geological Survey of Western Australia, Digital data layer, <www.dmirs.wa.gov.au/geophysics>.

Haines, PW 2011, Geological appraisal of petroleum exploration well Patience 2, Canning Basin, Western Australia: Geological Survey of Western Australia, Record 2011/11, 17p.

Hocking, RM 1994a, Basin subdivisions of Western Australia in Subdivisions of Western Australian Neoproterozoic and Phanerozoic sedimentary basins: Geological Survey of Western Australia, Record 1994/4, Plate 1.

Hocking, RM 1994b, Subdivisions of Western Australian Neoproterozoic and Phanerozoic sedimentary basins: Geological Survey of Western Australia, Record 1994/4, 85p.

Hunt Oil Company of Australia 1997, Final report, Waukarlycarly seismic survey interpretation; Hunt Oil Company of Australia: Geological Survey of Western Australia, Statutory petroleum exploration report S10316 A5 (open file).

Iasky, RP 1990, Officer Basin, in Geology and mineral resources of Western Australia: Western Australia Geological Survey, Memoir 3, p. 362–380.

Kennard, JM, Jackson, MJ, Romine, KK, Shaw, RD and Southgate, PN 1994, Depositional sequences and associated petroleum systems of the Canning Basin, WA, *in* The Sedimentary Basins of Western Australia *edited by* PG Purcell and RR Purcell: Petroleum Exploration Society of Australia, Western Australian Branch, Perth, Western Australia, p. 657–676.

Kopty, Z 2020, Downhole seismic logging, HiSeis Pty Ltd, WAPIMS, <https://wapims.dmp.wa.gov.au/WAPIMS/Search/WellDetails>.

Normore, LS and Rapaic, M 2020, Waukarlycarly 1 Basic Data Well Completion Report: Geological Survey of Western Australia; Geochronology Record Report 206: Geological Survey of Western Australia, 20p.

Ranasinghe, SP and Crosdale, PJ 2020, Report on source rock type, maturation levels and hydrocarbon potential of a suite of samples from Waukarlyarly-1 in the Canning Basin, Western Australia; Report prepared for Geoscience Australia: Geological Survey of Western Australia, Statutory petroleum exploration report G0004185A4, 20p.

Roach, IC, Costelloe, MT and Whitaker, AJ 2010, Previous and concurrent work, *in* Geological and energy implications of the Paterson airborne electromagnetic (AEM) survey, Western Australia *edited by* IC Roach: Geoscience Australia, Record 2010/12, p. 29–47.

Southby, C, Carr, L, Henson, P, Haines, P, Zhan, A, Anderson, J, MacFarlane, S, Fomin, T, Costelloe, R 2019, Exploring for the future: Kidson Sub-basin seismic interpretation: Australasian Exploration Geoscience Conference 2019.

Velseis Processing Pty Ltd (editor) 2019, Seismic Data Processing Report: 2018 Kidson Sub-basin Deep Crustal Seismic Survey, Land 2D, 42p.

Walker Petrophysics 2020, Petrpophysical Evaluation, Waukarlycarly 1: Walker Petrophysics Pty Ltd, WAPIMS, <https://wapims.dmp.wa.gov.au/WAPIMS/Search/WellDetails>.

Zhan, Y 2017, Canning Coastal seismic survey – an overview of the Canning Basin: Geological Survey of Western Australia, Record 2017/5, 29p.

Zhan, Y 2018, A seismic interpretation of the southwestern Canning Basin, Western Australia: Geological Survey of Western Australia, Report 178, 34p.

Zhan, Y 2019, A seismic interpretation of the Broome Platform, Willara Sub-basin and Munro Arch of the Canning Basin, Western Australia: Geological Survey of Western Australia, Report 193, 43p.

Zhan, Y and Haines, PW 2021, Kidson Sub-basin Seismic Survey – A panorama of the southern Canning Basin: Geological Survey of Western Australia, Report 216.

Zhan, Y and Mory, AJ 2013, Structural interpretation of the northern Canning Basin, Western Australia, *in* The Sedimentary Basins of Western Australia *edited by* M Keep and SJ Moss: West Australian Basins Symposium, Perth, 18–21 August 2013: Petroleum Exploration Society of Australia, 18p.

APPENDIX: Barnicarndy 1 VSP and checkshot data

VSP survey information	
Recording system	Wavelab II
Logging cable / cablehead	4C Rochester / GO
Receiver parameters	
Downhole tool	Sercel Slimwave 2-Level system
Receiver step	10 m
Sample length	2 s
Sample rate	1 ms
Record length	2 s
Source parameters	
Source type	Inova Univib (26 000 lbs)
Source control	Pelton VIBPRO
Operating force	70%
Source sweep	6-130 Hz linear sweep 15 s 300 ms cosine taper
Phase locking	Ground Force
Amplitude control	Peak to Peak
Source location ZVSP – Barnicarndy 1 (relative to collar)	Easting: 1 m
	Northing: 6 m
	ASL: 0 m

MD (m)	TVD (m)	Vertical time from source to reciver (ms; logged and interpreted by HiSeis)	Two-way vertical time (ms; logged and interpreted by HiSeis)	Pre-correction interval velocity (m/s; between geophones)	TWT (ms; revised to reduce anomalies in interval velocity; see Table 2 for explanation)	TWT (ms; after 215 ms upwards shift; see synthetic correlation in Figure 16)	Post-correction interval velocity (m/s; between geophones)	Post-correction average velocity (m/s; source to geophone)	Formation velocity (m/s)	Remarks
0.00	0.00	0.0	0.0		0.0	0.0				Ground/source
470.00	469.96	290.0	580.0	1621	585.6	370.6	2536	2536	3618 (Upper Grant Group: muddy diamictite, siltstone and sandstone)	Fair-quality checkshot
480.00	479.96	297.0	594.0	1429	592.1	377.1	3077	2546		
580.00	579.94	324.0	648.0	3703	649.0	434.0	3514	2673		
590.00	589.93	327.0	654.0	3330	654.8	439.8	3445	2683		
649.99	649.91	342.9	685.8	3772	685.7	470.7	3882	2761		
659.99	659.91	345.6	691.2	3704	691.1	476.1	3704	2772		Fair quality in VSP
669.99	669.91	348.3	696.6	3704	696.5	481.5	3704	2783		
679.99	679.91	350.9	701.8	3846	701.7	486.7	3846	2794		
689.99	689.91	353.6	707.2	3704	707.1	492.1	3704	2804		
699.99	699.91	356.4	712.8	3571	712.7	497.7	3571	2813		
709.99	709.90	358.9	717.8	3996	717.7	502.7	3996	2824	3219 (Lower Grant Group: low-porosity diamictite, mudstone, fine-grained sandstone)	Poor quality in VSP
719.99	719.90	362.4	724.8	2857	723.7	508.7	3333	2830		
729.99	729.90	365.9	731.8	2857	729.7	514.7	3333	2836		
739.99	739.90	368.9	737.8	3333	735.7	520.7	3333	2842		
749.99	749.90	369.9	739.8	10000	741.7	526.7	3333	2848		
759.99	759.90	372.2	744.4	4348	747.3	532.3	3571	2855		
769.99	769.90	374.8	749.6	3846	753.5	538.5	3226	2859		
779.99	779.90	376.8	753.6	5000	758.5	543.5	4000	2870		
789.98	789.89	379.0	758.0	4541	763.9	548.9	3700	2878		
799.99	799.89	382.5	765.0	2857	769.0	554.0	3922	2888		
809.99	809.89	387.2	774.4	2128	775.3	560.3	3175	2891		
819.99	819.89	391.8	783.5	2174	783.5	568.5	2439	2884		
829.99	829.89	396.3	792.7	2222	792.6	577.6	2198	2874		
839.99	839.89	400.9	801.8	2174	800.7	585.7	2469	2868		Good quality in VSP
849.99	849.89	403.3	806.6	4167	806.5	591.5	3448	2874		
859.99	859.89	406.1	812.2	3571	812.1	597.1	3571	2880		
869.98	869.88	408.6	817.2	3996	817.1	602.1	3996	2889	4092 (Upper Barnicarndy Formation: clean, well sorted, upper fine to lower coarse-grained quartz arenite)	
879.98	879.88	411.0	822.0	4167	821.9	606.9	4167	2900		
889.98	889.88	413.4	826.8	4167	826.7	611.7	4167	2910		
899.99	899.88	416.0	832.0	3846	831.9	616.9	3846	2917		
909.99	909.88	418.6	837.2	3846	837.1	622.1	3846	2925		
919.98	919.87	421.1	842.2	3996	842.1	627.1	3996	2934		
929.98	929.87	423.7	847.4	3846	847.3	632.3	3846	2941		
939.98	939.87	425.9	851.8	4545	851.7	636.7	4545	2952		
949.99	949.87	428.5	857.0	3846	856.9	641.9	3846	2960		
959.98	959.86	430.9	861.8	4163	861.7	646.7	4162	2968		
969.98	969.86	433.2	866.4	4348	866.3	651.3	4348	2978		
979.97	979.86	435.5	871.0	4348	870.9	655.9	4348	2988		

MD (m)	TVD (m)	Vertical time from source to reciver (ms; logged and interpreted by HiSeis)	Two-way vertical time (ms; logged and interpreted by HiSeis)	Pre-correction interval velocity (m/s; between geophones)	TWT (ms; revised to reduce anomalies in interval velocity; see Table 2 for explanation)	TWT (ms; after 215 ms upwards shift; see synthetic correlation in Figure 16)	Post-correction interval velocity (m/s; between geophones)	Post-correction average velocity (m/s; source to geophone)	Formation velocity (m/s)	Remarks
989.98	989.85	438.1	876.2	3842	876.1	661.1	3842	2995		
999.98	999.85	440.3	880.6	4545	880.5	665.5	4545	3005		
1009.97	1009.84	442.9	885.8	3842	885.7	670.7	3842	3011		
1019.98	1019.84	445.2	890.4	4348	890.3	675.3	4348	3020		
1029.97	1029.83	447.7	895.4	3996	895.3	680.3	3996	3028		
1039.97	1039.83	450.3	900.6	3846	900.6	685.6	3774	3033		
1049.98	1049.83	452.6	905.2	4348	905.1	690.1	4444	3043		
1059.97	1059.82	455.1	910.2	3996	910.2	695.2	3918	3049		
1069.98	1069.82	458.4	916.8	3030	915.5	700.5	3774	3054		
1079.97	1079.81	460.3	920.6	5258	920.6	705.6	3918	3061		
1089.98	1089.81	463.0	926.0	3704	926.0	711.0	3704	3066		
1099.97	1099.80	465.7	931.4	3700	931.4	716.4	3700	3070		
1109.98	1109.80	469.3	938.7	2778	936.7	721.7	3788	3076		
1119.97	1119.79	470.8	941.6	6660	941.6	726.6	4061	3082		
1129.97	1129.78	473.6	947.2	3568	947.2	732.2	3568	3086		
1139.97	1139.78	476.1	952.2	4000	952.1	737.1	4082	3093		
1149.97	1149.77	477.9	955.8	5550	955.8	740.8	5400	3104		
1159.97	1159.77	480.4	960.8	4000	960.8	745.8	4000	3110		
1169.97	1169.76	483.0	966.0	3842	966.0	751.0	3842	3115	4068 (Lower Barnicarndy Formation: well-sorted, lower fine to upper medium-grained quartz arenite)	Good quality in VSP
1179.97	1179.76	485.4	970.8	4167	970.8	755.8	4167	3122		
1189.97	1189.75	487.7	975.4	4343	975.4	760.4	4343	3129		
1199.97	1199.75	490.1	980.2	4167	980.1	765.1	4255	3136		
1209.98	1209.75	492.4	984.8	4348	984.7	769.7	4348	3143		
1219.97	1219.74	494.8	989.6	4162	989.5	774.5	4163	3150		
1229.98	1229.74	497.2	994.4	4167	994.3	779.3	4167	3156		
1239.97	1239.73	499.6	999.2	4162	999.1	784.1	4163	3162		
1249.97	1249.72	502.2	1004.4	3842	1004.3	789.3	3842	3167		
1259.97	1259.72	504.7	1009.4	4000	1009.3	794.3	4000	3172		
1269.97	1269.71	507.2	1014.4	3996	1014.3	799.3	3996	3177		
1279.97	1279.71	509.6	1019.2	4167	1019.1	804.1	4167	3183		
1289.98	1289.71	512.0	1024.0	4167	1023.9	808.9	4167	3189		
1299.97	1299.70	514.3	1028.6	4343	1028.5	813.5	4343	3195		
1309.97	1309.69	516.7	1033.4	4162	1033.3	818.3	4163	3201		
1319.97	1319.69	519.5	1039.0	3571	1038.9	823.9	3571	3204		
1329.97	1329.68	521.3	1042.6	5550	1042.5	827.5	5550	3214		
1339.97	1339.68	524.2	1048.4	3448	1048.3	833.3	3448	3215		
1349.97	1349.67	526.3	1052.6	4757	1052.5	837.5	4757	3223		
1359.97	1359.66	529.1	1058.2	3568	1058.1	843.1	3568	3225		
1369.97	1369.66	531.3	1062.6	4545	1062.5	847.5	4545	3232		

MD (m)	TVD (m)	Vertical time from source to reciver (ms; logged and interpreted by HiSeis)	Two-way vertical time (ms; logged and interpreted by HiSeis)	Pre-correction interval velocity (m/s; between geophones)	TWT (ms; revised to reduce anomalies in interval velocity; see Table 2 for explanation)	TWT (ms; after 215 ms upwards shift; see synthetic correlation in Figure 16)	Post-correction interval velocity (m/s; between geophones)	Post-correction average velocity (m/s; source to geophone)	Formation velocity (m/s)	Remarks
1379.97	1379.65	533.7	1067.4	4162	1067.3	852.3	4163	3237	3692 (Samphire Marsh Member of Nambeet Formation: mudstone)	
1389.97	1389.65	536.8	1073.6	3226	1073.5	858.5	3226	3237		Poor quality in VSP
1399.97	1399.64	541.1	1082.2	2323	1077.8	862.8	4647	3244		
1409.97	1409.64	541.0	1082.0	-100000	1081.9	866.9	4878	3252		
1419.97	1419.63	545.4	1090.8	2270	1090.7	875.7	2270	3242		
1429.97	1429.62	550.4	1100.8	1998	1098.7	883.7	2497	3236		
1439.97	1439.62	554.5	1109.0	2439	1103.7	888.7	4000	3240		
1449.97	1449.61	554.3	1108.7	-49950	1108.6	893.6	4078	3244		
1459.61	1459.61	560.3	1120.6	1667	1113.9	898.9	3774	3248		
1469.97	1469.60	561.1	1122.2	12487	1119.1	904.1	3842	3251		
1479.97	1479.60	562.8	1125.6	5882	1123.5	908.5	4545	3257		
1489.97	1489.59	563.1	1126.2	33300	1128.1	913.1	4343	3263		
1499.97	1499.59	566.3	1132.6	3125	1132.5	917.5	4545	3269		
1509.95	1509.57	570.0	1140.0	2697	1139.9	924.9	2697	3264		
1519.97	1519.58	573.5	1147.0	2860	1144.9	929.9	4004	3268		
1529.97	1529.58	573.6	1147.2	100000	1150.1	935.1	3846	3271		
1539.97	1539.57	579.2	1158.4	1784	1158.3	943.3	2437	3264		
1549.97	1549.57	581.6	1163.2	4167	1163.1	948.1	4167	3269		
1559.98	1559.57	583.0	1166.0	7143	1166.9	951.9	5263	3277		
1569.97	1569.56	584.2	1168.4	8325	1170.3	955.3	5876	3286		
1579.97	1579.56	587.3	1174.7	3226	1174.6	959.6	4651	3292		Good quality in VSP
1589.97	1589.55	591.6	1183.1	2323	1183.1	968.1	2351	3284		
1599.97	1599.55	593.3	1186.5	5882	1186.5	971.5	5882	3293		
1609.98	1609.55	595.2	1190.3	5263	1190.3	975.3	5263	3301		
1619.97	1619.54	598.1	1196.1	3445	1196.1	981.1	3445	3301		
1629.97	1629.54	601.1	1202.1	3333	1202.1	987.1	3333	3302		
1639.97	1639.53	603.8	1207.5	3700	1207.5	992.5	3700	3304		
1649.97	1649.53	606.9	1213.7	3226	1213.7	998.7	3226	3303		
1659.97	1659.53	609.6	1219.1	3704	1219.1	1004.1	3704	3306		
1669.97	1669.52	612.7	1225.3	3223	1225.3	1010.3	3223	3305		
1679.97	1679.52	615.5	1230.9	3571	1230.9	1015.9	3571	3306		
1689.98	1689.52	618.4	1236.7	3448	1236.7	1021.7	3448	3307		
1699.97	1699.51	621.2	1242.3	3568	1242.3	1027.3	3568	3309		
1709.97	1709.51	624.0	1247.9	3571	1247.9	1032.9	3571	3310		
1719.97	1719.50	626.7	1253.3	3700	1253.3	1038.3	3700	3312		
1729.96	1729.49	629.3	1258.5	3842	1258.5	1043.5	3842	3315		
1739.97	1739.49	632.0	1263.9	3704	1263.9	1048.9	3704	3317		
1749.96	1749.48	634.6	1269.1	3842	1269.1	1054.1	3842	3319		
1759.97	1759.48	637.6	1275.1	3333	1275.1	1060.1	3333	3319		

MD (m)	TVD (m)	Vertical time from source to reciver (ms; logged and interpreted by HiSeis)	Two-way vertical time (ms; logged and interpreted by HiSeis)	Pre-correction interval velocity (m/s; between geophones)	TWT (ms; revised to reduce anomalies in interval velocity; see Table 2 for explanation)	TWT (ms; after 215 ms upwards shift; see synthetic correlation in Figure 16)	Post-correction interval velocity (m/s; between geophones)	Post-correction average velocity (m/s; source to geophone)	Formation velocity (m/s)	Remarks
1769.96	1769.47	640.5	1280.9	3445	1280.9	1065.9	3445	3320		
1779.96	1779.46	643.4	1286.7	3445	1286.7	1071.7	3445	3321		
1789.96	1789.46	646.3	1292.5	3448	1292.5	1077.5	3448	3322		
1799.96	1799.45	649.3	1298.5	3330	1298.5	1083.5	3330	3322		
1809.96	1809.45	652.0	1303.9	3704	1303.9	1088.9	3704	3323		
1819.96	1819.44	655.0	1309.9	3330	1309.9	1094.9	3330	3323		
1829.95	1829.43	657.8	1315.5	3568	1315.5	1100.5	3568	3325		
1839.96	1839.43	660.5	1320.9	3704	1320.9	1105.9	3704	3327		
1849.95	1849.42	663.3	1326.5	3568	1326.5	1111.5	3568	3328		
1859.95	1859.41	665.9	1331.7	3842	1331.7	1116.7	3842	3330		
1869.95	1869.41	668.6	1337.1	3704	1337.1	1122.1	3704	3332		
1879.95	1879.40	671.3	1342.5	3700	1342.5	1127.5	3700	3334		
1889.95	1889.40	673.9	1347.9	3846	1347.8	1132.8	3774	3336		
1899.94	1899.39	676.6	1353.3	3700	1353.2	1138.2	3700	3338		
1909.94	1909.38	679.3	1358.7	3700	1358.6	1143.6	3700	3339		
1919.94	1919.38	681.8	1363.7	4000	1363.6	1148.6	4000	3342		
1929.94	1929.37	684.5	1369.1	3700	1369.0	1154.0	3700	3344		
1939.94	1939.37	687.2	1374.5	3704	1374.4	1159.4	3704	3345		
1949.94	1949.36	690.6	1381.3	2938	1381.2	1166.2	2938	3343		
1959.93	1959.35	693.3	1386.7	3700	1386.6	1171.6	3700	3345	3692 (Samphire Marsh Member of Nambeet Formation: mudstone)	Good quality in VSP
1969.94	1969.35	695.9	1391.9	3846	1391.8	1176.8	3846	3347		
1979.93	1979.34	698.5	1397.1	3842	1397.0	1182.0	3842	3349		
1989.94	1989.34	701.3	1402.7	3571	1402.6	1187.6	3571	3350		
1999.93	1999.33	703.9	1407.9	3842	1407.8	1192.8	3842	3352		
2009.93	2009.32	706.7	1413.5	3568	1413.4	1198.4	3568	3353		
2019.93	2019.32	709.2	1418.5	4000	1418.4	1203.4	4000	3356		
2029.93	2029.31	711.8	1423.7	3842	1423.6	1208.6	3842	3358		
2039.93	2039.31	714.4	1428.9	3846	1428.8	1213.8	3846	3360		
2049.93	2049.30	717.1	1434.3	3700	1434.2	1219.2	3700	3362		
2059.92	2059.29	719.6	1439.3	3996	1439.2	1224.2	3996	3364		
2069.93	2069.29	722.3	1444.7	3704	1444.6	1229.6	3704	3366		
2079.92	2079.28	724.9	1449.9	3842	1449.8	1234.8	3842	3368		
2089.91	2089.27	727.5	1455.1	3842	1455.0	1240.0	3842	3370		
2099.92	2099.27	730.2	1460.5	3704	1460.4	1245.4	3704	3371		
2109.91	2109.26	732.9	1465.9	3700	1465.8	1250.8	3700	3373		
2119.92	2119.26	735.5	1471.0	3846	1471.0	1256.0	3846	3375		
2129.91	2129.25	738.3	1476.6	3568	1476.6	1261.6	3568	3375		
2139.91	2139.24	741.0	1482.0	3700	1482.0	1267.0	3700	3377		
2149.91	2149.24	743.5	1487.0	4000	1487.0	1272.0	4000	3379		

MD (m)	TVD (m)	Vertical time from source to reciver (ms; logged and interpreted by HiSeis)	Two-way vertical time (ms; logged and interpreted by HiSeis)	Pre-correction interval velocity (m/s; between geophones)	TWT (ms; revised to reduce anomalies in interval velocity; see Table 2 for explanation)	TWT (ms; after 215 ms upwards shift; see synthetic correlation in Figure 16)	Post-correction interval velocity (m/s; between geophones)	Post-correction average velocity (m/s; source to geophone)	Formation velocity (m/s)	Remarks
2159.91	2159.23	746.1	1492.2	3842	1492.2	1277.2	3842	3381	3692 (Samphire Marsh Member of Nambeet Formation: mudstone)	Good quality in VSP
2169.91	2169.23	748.8	1497.6	3704	1497.6	1282.6	3704	3383		
2179.91	2179.22	751.4	1502.8	3842	1502.8	1287.8	3842	3384		
2189.90	2189.21	754.0	1508.0	3842	1508.0	1293.0	3842	3386		
2199.91	2199.21	756.7	1513.4	3704	1513.4	1298.4	3704	3388		
2209.90	2209.20	759.5	1519.0	3568	1519.0	1304.0	3568	3388		
2219.91	2219.20	762.1	1524.2	3846	1524.2	1309.2	3846	3390		
2229.90	2229.19	764.9	1529.8	3568	1529.8	1314.8	3568	3391		
2239.90	2239.18	767.4	1534.8	3996	1534.8	1319.8	3996	3393		
2249.90	2249.18	770.0	1540.0	3846	1540.0	1325.0	3846	3395		
2259.90	2259.17	772.5	1545.0	3996	1545.0	1330.0	3996	3397		
2269.90	2269.17	775.3	1550.6	3571	1550.6	1335.6	3571	3398		
2279.89	2279.16	777.9	1555.8	3842	1555.8	1340.8	3842	3400	4253 (Fly Flat Member of Nambeet Formation: very fine to fine-grained low-porosity sandstone)	
2289.89	2289.15	780.4	1560.8	3996	1560.8	1345.8	3996	3402		
2299.89	2299.15	783.3	1566.6	3448	1566.6	1351.6	3448	3402		
2309.89	2309.14	785.1	1570.2	5550	1570.2	1355.2	5550	3408		
2319.88	2319.13	787.2	1574.4	4757	1574.4	1359.4	4757	3412		
2329.89	2329.13	789.9	1579.8	3704	1579.7	1364.7	3774	3413		
2339.88	2339.12	792.4	1584.8	3996	1584.7	1369.7	3996	3416		
2349.89	2349.12	794.8	1589.6	4167	1589.5	1374.5	4167	3418		
2359.88	2359.11	796.9	1593.8	4757	1593.7	1378.7	4757	3422		
2369.88	2369.10	799.4	1598.8	3996	1598.7	1383.7	3996	3424		
2379.88	2379.10	801.4	1602.8	5000	1602.7	1387.7	5000	3429		
2389.88	2389.09	804.1	1608.2	3700	1608.1	1393.1	3700	3430		
2399.88	2399.09	806.6	1613.2	4000	1613.1	1398.1	4000	3432		
2409.88	2409.08	809.0	1618.0	4162	1617.9	1402.9	4162	3434		
2419.87	2419.07	811.3	1622.6	4343	1622.5	1407.5	4343	3437		
2429.88	2429.07	813.6	1627.2	4348	1627.1	1412.1	4348	3440		
2439.87	2439.06	814.8	1629.6	8325	1630.5	1415.5	5876	3446		
2449.88	2449.06	816.9	1633.8	4762	1633.7	1418.7	6250	3453	4836 (Yapukarninjarra Formation: medium to coarse-grained quartz arenite)	
2459.87	2459.05	818.9	1637.8	4995	1637.7	1422.7	4995	3457		
2469.87	2469.04	821.6	1643.2	3700	1643.1	1428.1	3700	3458		
2479.87	2479.04	823.6	1647.2	5000	1647.1	1432.1	5000	3462		
2489.86	2489.03	826.2	1652.4	3842	1652.3	1437.3	3842	3463		
2499.86	2499.02	828.6	1657.2	4162	1657.1	1442.1	4162	3466		
2509.86	2509.02	830.4	1660.8	5556	1660.7	1445.7	5556	3471		
2519.86	2519.01	833.2	1666.4	3568	1665.4	1450.4	4251	3474		
2529.88	2529.03	834.8	1669.6	6263	1669.5	1454.5	4888	3478		
2539.86	2539.00	836.4	1672.7	6231	1672.7	1457.7	6231	3484		

MD (m)	TVD (m)	Vertical time from source to reciver (ms; logged and interpreted by HiSeis)	Two-way vertical time (ms; logged and interpreted by HiSeis)	Pre-correction interval velocity (m/s; between geophones)	TWT (ms; revised to reduce anomalies in interval velocity; see Table 2 for explanation)	TWT (ms; after 215 ms upwards shift; see synthetic correlation in Figure 16)	Post-correction interval velocity (m/s; between geophones)	Post-correction average velocity (m/s; source to geophone)	Formation velocity (m/s)	Remarks
2549.85	2548.99	838.3	1676.5	5258	1676.5	1461.5	5258	3488	4836 (Yapukarninjarra Formation: medium to coarse-grained quartz arenite)	Good quality in VSP
2559.86	2558.99	840.0	1679.9	5882	1679.9	1464.9	5882	3494		
2569.86	2568.99	841.7	1683.3	5882	1683.3	1468.3	5882	3499		
2579.86	2578.98	844.1	1688.1	4163	1688.1	1473.1	4163	3501		
2589.85	2588.97	846.3	1692.5	4541	1692.5	1477.5	4541	3505		
2599.85	2598.96	848.2	1696.3	5258	1696.3	1481.3	5258	3509	4797 (basement: weakly metamorphosed dolomitic siltstone below weathered regolith)	
2609.85	2608.96	850.4	1700.7	4545	1700.7	1485.7	4545	3512		
2619.85	2618.95	852.5	1705.0	4757	1705.0	1490.0	4647	3515		

Record 2021/9

Geophysical analysis of Barnicarndy 1: data quality control, velocity anomalies, out-of-plane reflections, and correlation uncertainties

Y Zhan

Access GSWA products

All products
All GSWA products are free to download as PDFs from the DMIRS eBookshop <www.dmirs.wa.gov.au/ebookshop>. View other geoscience information on our website <www.dmirs.wa.gov.au/gswa>.

Hard copies
Limited products are available to purchase as hard copies from the First Floor counter at Mineral House or via the DMIRS eBookshop <www.dmirs.wa.gov.au/ebookshop>.

Fieldnotes
Fieldnotes is a free digital-only quarterly newsletter which provides regular updates to the State's exploration industry and geoscientists about GSWA's latest programs, products and services. Access by subscribing to the GSWA eNewsletter <www.dmirs.wa.gov.au/gswaenewsletter> or downloading the free PDF from the DMIRS eBookshop <www.dmirs.wa.gov.au/ebookshop>.

GSWA eNewsletter
The GSWA eNewsletter is an online newsletter that contains information on workshops, field trips, training and other events. To keep informed, please subscribe <www.dmirs.wa.gov.au/gswaenewsletter>.

Further details of geoscience products are available from:

First Floor Counter
Department of Mines, Industry Regulation and Safety
100 Plain Street
EAST PERTH WESTERN AUSTRALIA 6004
Phone: +61 8 9222 3459 Email: publications@dmirs.wa.gov.au
www.dmirs.wa.gov.au/GSWApublications